KYAMBOGO UNIVERSITY

PERFORMANCE OF PLASTIC-DERIVED LIQUID FUEL IN A COMPRESSION IGNITION ENGINE

BY

WAISWA TIFU

17/U/14836/GMSP/PE

A DISSERTATION SUBMITTED TO THE DIRECTORATE OF RESEARCH AND GRADUATE TRAINING IN PARTIAL FULFILMENT OF THE REQUIREMENTS FOR THE AWARD OF THE DEGREE OF MASTER OF SCIENCE IN PHYSICS OF KYAMBOGO UNIVERSITY

SEPTEMBER 2023

Declaration

I, **Waiswa Tifu**, declare that the work contained in this dissertation was done by me and has not been submitted to any University for consideration of an academic award.

Signature: .....

Date: .....

Approval

This is to certify that the work covered in this dissertation by Waiswa Tifu was designed and carried out under our supervision. The dissertation is now ready for presentation to the Board of Graduate School and Senate of Kyambogo University.

Signature: .....

First Supervisor: Dr. Okullo Michael

Date: .....

Signature: .....

Second Supervisor: Prof. Edward Jurua

Date: .....

Dedication

To my beloved ones.

Acknowledgement

I thank the Almighty ALLAH for making it possible for me to finish my dissertation and for giving me all the resources I needed.

I would like to thank my supervisors, Dr. Okullo Michael and Prof. Edward Jurua, from the bottom of my heart for their continuous assistance and helpful advice during the time of this study.

My sincere thanks go to the Management and staff of Ministry of Energy and Mineral Development, particularly the petroleum department, for all the assistance, and guidance they rendered to me in the analysis of the fuel samples. I thank Spero Byokunda (PhD), Ivan Okumu, Christine Kabajungu, and Gilbert Tukei for their help in the determination of the quality parameters of liquid fuel.

I am grateful to the Department of Mechanical and Production Engineering, Kyambogo University, especially Okumu Otebi Lawrence, Ochola Samson Opige, and Ongora Solomon for the assistance offered in evaluating the performance of the fuel samples in a diesel engine.

Special thanks go to my wife, Ssubi Dorcus, for the help she gave me, especially for taking care of our children while I was away. Very special thanks go to my dear children Kirabo Sonia Priscilla, Mwebaza Rania Sofia, and Mukisa Ramathan Mesuit for the endurance of my absence when they missed my presence for a long time.

In addition, I thank Kyambogo University, Department of Physics for the support and all the provisions, and to everyone who assisted me in completing this dissertation.

Table of Contents

List of Figures

List of Tables

List of Acronyms

ASTM American Society for Testing and Materials

BP Brake Power

BSFC Brake Specific Fuel Consumption

BTE Brake Thermal Efficiency

CCI Calculated Cetane Index

CI Compression Ignition

HDPE High-Density Polyethylene

HDPELF High-Density Polyethylene Liquid Fuel

IC Internal Combustion

ISFC Indicated Specific Fuel Consumption

ISO International Organization for Standardization

IP Indicated Power

LDPE Low-Density Polyethylene

LLDPE Linear Low-Density Polyethylene

PE Polyethylene

PET Polyethylene Terephthalate

PP Polypropylene

PPLF Polypropylene Liquid Fuel

PS	Polystyrene
PVC	Polyvinyl Chloride
SDG	Sustainable Development Goal
SFC	Specific Fuel Consumption
SI	Spark Ignition
UNBS	Uganda National Bureau of Standards

Abstract

Fossil fuels are the major sources of energy for running engines, powering industries, and for supporting domestic activities. However, as energy-intensive activities increase, there is a need for diverse sources of energy other than petroleum-based sources. This has led to the production of alternative liquid fuels from industrial waste, residential waste, agricultural waste, and plastics. Such fuels have been characterized and compared to petroleum fuels. However, additional testing of these fuels in engines reveals more data regarding the quality of these fuels in relation to the power of the engine. This study was designed to produce fuel from two types of plastics, High-Density Polyethylene (HDPE) and Polypropylene (PP) plastics through thermal pyrolysis, characterize the obtained liquid fuels, and evaluate their performance in a diesel engine in relation to standard diesel. The density of the fuel samples were measured to be 0.830 ± 0.001, 0.790 ± 0.003 and 0.788 ± 0.001 g cm^{-3}, ash content was 0.02 ± 0.01, 0.03 ± 0.01 and 0.02 ± 0.00 % (m/m), cetane index was 53, 65 and 66, copper strip corrosion was class 1a, class 3a, and class 1a, kinematic viscosity of 2.71 ± 0.04, 2.00 ± 0.04 and 2.04 ± 0.02 cSt, and calorific value was 47.59 ± 0.49, 48.65 ± 0.13 and 48.52 ± 0.00 MJ/kg for standard diesel, High-Density Polyethylene Liquid Fuel (HDPELF) and Polypropylene Liquid Fuel (PPLF) respectively. The engine tests revealed that liquid fuel from HDPE and PP plastics had 12.8 % and 10.7 % higher Brake Specific Fuel Consumption, and a lower Brake Power of 1.3 % and 2.3 % respectively than that of standard diesel. The Brake Thermal Efficiency of HDPELF and PPLF were found to be 15.2 % and 13.1 % lower than when using standard diesel. These results suggest that the liquid fuel obtained from HDPE and PP plastic can be used as fuels in diesel engines with a minimum drop in brake power.

Chapter 1

Introduction

1.1 Background of the Study

One of the most essential components for heating, lighting, and transportation is energy. Energy is also used for domestic and commercial activities. The world's population is expanding and the economy is progressing, which is causing an increase in energy demand. Fuel demand grew, and in 2021 fossil fuels provided approximately 85% of the energy used worldwide (Sayyed et al., 2021). More energy must be produced from a variety of sources as energy-intensive activities increase. The production of biodiesel from biomass is the subject of current research (Bulushev and Ross, 2018). This is made from basic ingredients that are also used to feed people, which depletes food supplies. However, other technologies allow the manufacture of bio-diesel from crops that cannot be consumed by humans, such as the seeds of jatropha curcas, castor trees, and some energy crops (e.g Soybean, rapeseed, sunflower, and palm) that are planted particularly for energy production. It can also be made from industrial, residential, agricultural wastes, tyres, and plastics. (Macharia, 2018).

Plastics are one of the most widely utilized materials globally. This is because of their thermal, chemical, and mechanical qualities. In comparison to 2018's productivity of 359 million tons, global plastic production increased by 2.4 % in 2019 to 368 million tons (Tiseo, 2021). As a result, there is a growing amount of plastic waste. These materials are petroleum derivatives with heat values comparable to fossil fuels (Baines, 1993). The production of plastic waste in 2016 was estimated at 242 million tons by the World Bank, accounting for 12 % of municipal refuse, and by 2025, that percentage is expected to

rise to 13 % (Tsakona and Rucevska, 2020). Plastic is considered as one of the abundant sources from which alternative fuels can be generated. One technology for reclaiming energy from plastic materials is pyrolysis. In the absence of oxygen, this causes polymers to degrade by splintering big hydrocarbon chains into smaller ones resulting into liquid, gas, and solid products.

The possibility of recycling plastics for energy production has been studied. Dobó et al. (2019) conducted thermal pyrolysis experiments using High-Density polyethylene (HDPE), Low-Density Polyethylene (LDPE), PP, Polystyrene (PS), and Polyethylene Terephthalate (PET) plastics. The fuel obtained was refined by atmospheric distillation at 200 °C to obtain transport fuels, to a yield of 37.3 %, 40.8 %, 42.1 % and 70.5 % gasoline. The opportunity of recovering crude fuel from PP, HDPE and LDPE was studied by Tulashie et al. (2019) in a fixed bed reactor at 350 °C. The kinematic viscosity of the acquired fuel was determined to be 1.036 cSt and this parameter was reduced with an increase in temperature. Quesada et al. (2019) focused on density, cetane index, and kinematic viscosity to assess the quality of fuel obtained from Polyethylene plastic film through pyrolysis. The physical properties were very similar to those of commercial fuels such as diesel and gasoline. However, the fuel obtained was not evaluated in internal combustion engines to assess its performance in terms of engine power production.

More research has been done and it is being done to produce transport fuels from plastics, and biomass. These fuels have been characterized based on their physical and chemical properties. The quality of the fuel being used is one of the crucial elements that affect how Internal Combustion (IC) engines operate. There are three different types of internal combustion engines depending on how the fuel is ignited: use of spark plugs, injectors and hot spots. While the Compression Ignition (CI) engine uses diesel, the Spark Ignition (SI) engine runs on gasoline (Heywood, 2018). Such engines can also run on biofuels, ethanol, used lubricating oil, and fuels derived from waste plastics and/or discarded tyres. Little has been done to assess how well these fuels operate in IC engines to understand their quality in relation to engine power.

The quality of petroleum fuels has become more significant in terms of emission and combustion characteristics, as well as their efficiency in IC engines. This is primarily

driven by the rising demand for fuels that address environmental concerns. As a result, international standards set by organizations such as the International Organization for Standardization (ISO) have established requirements for alternative liquid fuels to meet the same standards as traditional transportation fuels in order to be considered viable options for the market(ASTM, 2003). Chemical analysis or fuel property measurements can be used to assess the quality of liquid fuels. Further testing of this fuel in conventional diesel and gasoline engines may reveal more about their quality in relation to engine power in terms of emission and combustion characteristics. Therefore, it is crucial to determine whether liquid fuel from plastics is appropriate for use in IC engines.

1.2 Statement of the Problem

Liquid fuel from plastics has been produced and characterized, which may then be used for generating energy in various ways including running internal combustion engines. The use of plastic-derived liquid fuel in internal combustion engines offers a promising avenue for sustainable and environmentally friendly energy solutions. However, the performance characteristics of plastic-derived liquid fuel in internal combustion engines remain relatively unexplored. This study investigated and evaluated engine performance using plastic-derived liquid fuel in a CI engine. This was compared to standard diesel, focusing on power output, thermal efficiency, and specific fuel consumption in order to determine whether such fuels can as well serve as viable alternatives to petroleum fuels.

1.3 Purpose of the Study

To assess the performance of plastic-derived liquid fuel in a compression ignition engine.

1.4 Objectives of the Study

(i) To produce liquid fuel from plastics using a fabricated pyrolysis reactor.

(ii) To determine the properties of the plastic-derived liquid fuel and standard diesel fuel sold in the market.

(iii) To compare the performance of plastic-derived fuel to standard diesel fuel sold in the market.

1.5 Scope of the Study

The focus of the study was the production of liquid fuel from HDPE and PP plastics using thermal pyrolysis in a fabricated pyrolysis system, characterizing the fuel, and assessing how well it operates in a single-cylinder, 4-stroke water-cooled diesel engine in relation to standard diesel, in terms of brake power, brake specific fuel consumption and brake thermal efficiency.

1.6 Significance of the Study

Investigating the performance of liquid fuel made from plastics in a CI engine addresses Sustainable Development Goal (SDG) 7, which aims to ensure access to affordable, reliable, sustainable, and modern energy for all. This alternative fuel can potentially reduce dependency on fossil fuels, contribute to cleaner energy solutions, and enhance energy security.

The study explores an innovative approach to converting plastic waste into a usable fuel source, aligning with SDG 9. This goal focuses on promoting sustainable industrialization and fostering innovation to build resilient infrastructure and encourage sustainable practices.

The study aligns with Uganda's long-term development vision, which seeks to transform the country into a middle-income country and ensure sustainable development by 2040. Integrating alternative fuels like liquid fuel made from plastics can support Uganda's efforts to diversify its energy sources and promote environmentally friendly practices.

Chapter 2

Review of related literature

2.1 Introduction

This chapter reviews the types of plastics as well as the process for converting plastics to liquid fuel. It reviews the properties of standard diesel as a conventional fuel for CI engines; as well as liquid fuel from plastics. Finally, it discusses the engine performance parameters in relation to combustion characteristics.

2.2 Types of plastics

The term "plastic" originates from the Greek word "plasticos," which means to shape or mold and it refers to the ability of a substance to take on different forms. A polymer, a Greek term in which "poly" means numerous and "mer" means unit, is another name for plastics. As a result, plastics are materials that can be moulded into a variety of shapes and are made up of lengthy chains of repeated large units (Bradfield, 2014). Depending on their structure, polymers can be categorized as linear, branched, or cross-linked, giving two types of plastics: thermoplastics and thermosetting (Bradfield, 2014). The difference between thermoplastics and thermosetting is determined by cross-linking. A polymer is considered to be thermosetting if it has cross-links because it breaks down before melting. These are unsuitable for recycling under thermal processing because they can melt when heated and only assume shape once. However, branching and linear polymers melt before the temperatures required for breaking down the polymer chains. Thermoplastic is the name given to these polymers. Upon exposure to adequate heat, these plastics undergo a transition into a softened and molten state. Subsequently, as they cool down, they solid-

ify to a degree that renders them sufficiently rigid for the purpose of manufacturing new plastics (Padsalgikar, 2017). PP, PS, Polyvinyl Chloride (PVC), and Polyethylene, PE (HDPE, LDPE, Linear Low-Density Polyethylene (LLDPE), and PET) are the few examples of thermoplastics (Chomba, 2018). To help customers and recyclers categorize the various types of plastics, the Society of Plastic Manufactures in 1988 introduced numbers (codes) which are molded at the bottom of every plastic produced (Council, 2017). The codes also provide information about the specific type of plastic resin used in the manufacturing of a particular plastic, recycling compatibility, sorting and separation, material property, and safety considerations (Council, 2017). Figure 2.1 shows how these codes correspond to a particular type of plastic.

Figure 2.1: Types of plastics based on Resin Identification number

Plastics are materials derived from petroleum products and they have heat values that are comparable to fossil fuels as shown in Figure 2.2 (Baines, 1993).

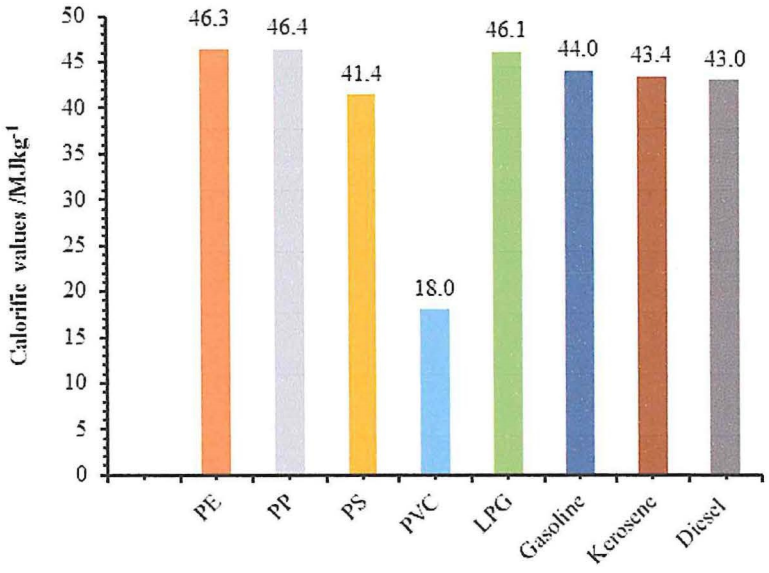

Figure 2.2: Calorific values of petroleum products and plastics (Baines, 1993)

2.3 Production of Fuel from Plastics

There are numerous methods for recovering energy from plastics. One of these is pyrolysis, which breaks down plastics into smaller hydrocarbon chains in the absence of oxygen, preventing the creation of oxides of carbon, sulfur, and nitrogen (Joshi et al., 2015). As a result of this process, liquid fuel, char, and non-condensable gases are produced. The pyrolysis method can either be thermal or catalytic, and these are discussed in the following subsections.

2.3.1 Thermal Pyrolysis

When a plastic substance is heated in an inert atmosphere, a process known as thermal pyrolysis takes place. During this process, the organic component of the plastic polymer material is broken down, and liquids and gases are produced that can be used as fuel and/or raw materials. This method is suitable for a complex polymer that contains a number of highly mixed materials (Mangesh et al., 2017).

During thermal pyrolysis, the plastic material is placed in a reactor, where it is heated. Hydrocarbons including linear and branched-chain aliphatic and aromatic hydrocarbons are obtained through condensing the pyrolytic vapour that travels through the associated condenser units (Suresh et al., 2018). To obtain crude oil, it is necessary to remove oxygen from the pyrolysis reactor, evenly distribute and control the heat applied to the reactor, continuous stirring to manage the solid product before it functions as a thermal insulator, and condense the vapour from the reactor (Suresh et al., 2018). This method produces useful products, that is liquids and gases (Singh et al., 2011).

Dobó et al. (2019), Brebu et al. (2004), Tulashie et al. (2019), and Sakata et al. (1996) obtained liquid fuel from HDPE, PP, LDPE, PS, PET, and Polyurethane (PUR) plastics and a mixture of such plastics through thermal pyrolysis. Their studies reveal that the liquid fuel yield is highest at pyrolysis temperatures between 400 ^{o}C and 450 ^{o}C. The obtained liquid fuel was characterized and it was found that it conforms to standard diesel based on the kinematic viscosity, density, and calorific value determined in the study.

2.3.2 Catalytic Pyrolysis

Catalytic pyrolysis involves heating a substance in the presence of catalysts in an inert environment. The organic element of the plastic polymer material decomposes in this process, generating gases and liquids (Mangesh et al., 2017). Synthetic polymers are man-made macro-molecules composed of repeating units called monomers. Synthetic polymers are created through chemical reactions, typically involving the polymerization of monomers and they are widely used in various industries and everyday products due to their customizable properties and versatility. Synthetic polymers degrade at temperatures between 350 °C to 550 °C in an endothermic process that requires a lot of heat. High temperatures of 700 °C to 900 °C have been used in other studies with the successful production of liquid fuel, solid, and gases (Demirbas, 2004). In contrast to thermal degradation, catalytic degradation may be done at low temperatures and yields high-quality products. (Miskolczi et al., 2004). The cost of thermal energy can be reduced and product yields can be increased through the use of efficient catalysts to lower these temperatures.

Owusu et al. (2018), produced liquid fuel from HDPE, PP, and PS plastics through thermal and catalytic pyrolysis. The results showed that the pyrolysis temperature for HDPE, PP, and PS plastics was higher at 450 °C, 350 °C, and 300 °C respectively without a catalyst, and lower at 300 °C, 270 °C, and 250 °C with silica-alumina catalyst. The degradation temperature for HDPE, PP, and PS was reduced by about 33 %, 23 %, and 17 %, respectively with the use of a catalyst. The density of liquid fuel from HDPE, PP, and PS was 796 kg m^{-3}, 786 kg m^{-3}, and 894 kg m^{-3}, kinematic viscosities of 2.373 cSt, 2.115 cSt and 1,46 cSt, a range of boiling points from 119 to 364 degrees Celsius and 148 to 355 degrees Celsius, as well as a cetane index of 46 and 63, respectively. Based on these properties, the liquid fuel from HDPE and PP plastics conform to standard diesel specifications. Therefore, there is a need to test such fuels in IC engines in comparison to standard diesel to reveal more information in terms of power generated by the engine.

Moses (2014) obtained liquid fuel from HDPE and LDPE plastics through catalytic pyrolysis using 10 % silica-alumina as a catalyst and 10 % sodium carbonate as a scavenger. The two primary factors that affected the production process were residence time and temperature. To assess the quality of the fuel obtained, the density and kinematic viscos-

ity were determined as 785 kg m^{-3}, and 2.18 cSt, and cetane number in the range of 62 - 64 respectively. The liquid fuel conforms to standard diesel but needs to be assessed in a CI engine in terms of power production.

Natural catalysts such as Shwedaung clay, Mabisan clay, Bentonite clay, Dolomite, and synthetic catalysts such as zinc oxide, were used by Kyaw and Hmwe (2015) to pyrolyze 200 g of mixed HDPE, LDPE, PS, PP PET plastics in a fixed bed reactor. The highest yield was attained from mixed plastics using Mabisan clay in a temperature range of 220 °C to 370 °C after 1 hour and 30 minutes. The study reported 703.6 kg m^{-3} and 2.82 cSt as the density and kinematic viscosity of the fuel obtained using Mabisan clay catalysts.

Altohami and Mustafa (2018) subjected a mixture of PP and LDPE plastics to thermal degradation using different amounts of kaolin as a catalyst in the production of liquid fuel. Under laboratory conditions, the density of the fuel produced was calculated as 795 kg m^{-3}, and viscosity was measured as 5.684 cSt. The viscosity value obtained is higher than the values in the study of Kyaw and Hmwe (2015). This may be attributed to the amount and type of catalyst used by Altohami and Mustafa (2018).

Using Natural zeolites catalysts, Coniwanti et al. (2020) found out that 300 g material ratio of 30:70 of LDPE:HDPE plastics produced 0.083 litres of liquid fuel at 400 °C, with kinematic viscosity of 1.15735 cSt, density of 0.770 g cm^{-3}, and heat value of 43.03 MJ kg^{-1}. The produced fuel had lower kinematic viscosity and lower density as compared to the fuel obtained by Moses (2014), Kyaw and Hmwe (2015), and Altohami and Mustafa (2018).

2.4 Properties of fuel for Compression Ignition engines

All fuels must conform to certain requirements in order to be used in compression ignition engines (Macharia, 2018). The following section discusses the key fuel characteristics and how they affect these engines.

2.4.1 Density

This is an important quantity that, in conjunction with other characteristics, can be used to characterize the heavy and light fractions of petroleum fuels. It is also important to determine the density of petroleum products in order to convert measured volumes to mass at a standard temperature of 15 °C (George et al., 2003). Whereas density is a quality-determining parameter of liquid fuels, it is an uncertain indicator of fuel quality except when it is correlated with other properties such as kinematic viscosity, cetane index, ash content, calorific value e.t.c.(George et al., 2003).

Density is calculated at a constant temperature because a liquid's volume changes with temperature (ASTM, 2003). For figuring out how dense liquid petroleum products are, there are two standard approaches: the automated oscillating tube apparatus used in ASTM D 4052 and ASTM D 1298 using a hydrometer (George et al., 2003). In ASTM D 1298 standard method, a single transparent 100 ml glass measuring cylinder is filled with 100 ml of the fuel sample and maintained at the test temperature. A hydrometer and a thermometer are lowered into the fuel sample and are then used to measure the fuel density and the test temperature respectively. According to ASTM D1298, the standard density of diesel lies in the range of 0.820 g cm^{-3} to 0.870 g cm^{-3} as indicated in table 2.1.

2.4.2 Copper strip corrosion

This is a significant parameter that is used to assess the relative degree of corrosivity of petroleum products due to active sulfur compounds (Malinović et al., 2022). The copper Corrosion test is a widely used oil analysis method for gearbox, turbine, and hydraulic lubricants (Jain et al., 2020). This oil analysis method detects the corrosive effects of a lubricant on copper alloys, but it is ineffective on iron or ferrous alloy parts and components.

The copper corrosion oil analysis method, ASTM D130, is relatively simple. A polished copper strip is immersed in 30 ml of the sample at elevated temperature, 50 °C or 100° C, depending on the type of gasoline, grease, or oil tested, for a period of three hours (ASTM, 2003). At the end of this period, the copper strip is cleaned and examined for evidence of degradation. Results are rated by comparing the stains on the copper strip to

the ASTM color-match scale from 1a to 4c (Sabarinath et al., 2019) as shown in Figure 2.3.

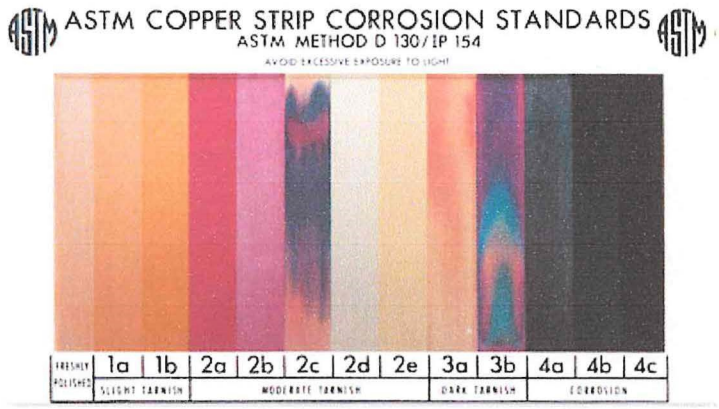

Figure 2.3: Copper strip corrosion standards

Class 1, the copper strip shows no visible signs of corrosion, indicating that the tested sample is non-corrosive towards copper. Class 2, the copper strip may exhibit slight discoloration or surface tarnish, but there is no significant corrosion or loss of copper. Class 3, moderate corrosion is observed on the copper strip, typically characterized by distinct tarnish, discoloration, or pitting. However, there is no complete loss of copper. Class 4, the copper strip undergoes severe corrosion, including substantial loss of copper and possible formation of copper salts or compounds (Sabarinath et al., 2019).

2.4.3 Kinematic Viscosity

Kinematic viscosity is a measure of a fluid's resistance to flow under the influence of gravity. It specifically refers to the fluid's internal friction to shear forces. In the context of petroleum fuels, kinematic viscosity is a fundamental property that characterizes the fuel's flow behavior and determines its ability to lubricate and transfer energy within a system (Nadkarni and Nadkarni, 2007). The appropriate viscosity of the fuel utilized is crucial to the efficient functioning of machines. Most petroleum fluids have a kinematic viscosity that can be estimated by determining the best conditions for storing, transporting, and operating with the fluid in question. For this reason, many product standards rely on a precise measurement of kinematic viscosity (ASTM, 2003). A proper ratio of fuel to air is required for a fuel to burn completely. Injection requires atomizing the fuel into tiny droplets so that it can penetrate and spread out evenly throughout the combustion chamber (Macharia, 2018). The quality of the spray from an injector is determined by

the fuel's viscosity. There will be less atomization and deeper penetration of the droplets during injection if the fuel has a high viscosity and as a result, the combustion process is interrupted. Low viscosity improves atomization at the injector nozzle but reduces penetration. Power production reduces at both viscosity extremes due to air-to-fuel ratio inconsistencies (George et al., 2003).

According to George et al. (2003), kinematic viscosity also has an impact on the lubrication and durability of the components of a fuel system. This is in addition to its impact on the combustion process. Wright and Purday (1950) explained that the engine fuel system depends on the lubrication of the operating fuel, very low viscosity fuels have poor lubrication qualities, which could lead to wear on the fuel pump and injector elements. The higher the temperature, the less viscous the fuel is; implying that viscosity changes with temperature. It must therefore be reported at a specific temperature. According to ASTM D445, the minimum and maximum working limits for the kinematic viscosity of conventional diesel should be 2.0 and 5.3 cSt at 40 °C to ensure adequate lubrication without stressing the injector parts (Macharia, 2018).

2.4.4 Distillation Characteristics

The distillation characteristics of fuels exert a great influence on performance (George et al., 2003). The distillation curve of a liquid fuel provides insight into its volatility. Any liquid fuel's distillation property greatly affects its efficiency. For fuels and solvents in particular, the volatility properties of hydrocarbons have a major impact on their efficiency and safety. The boiling point distribution can be used to identify the different fuel fractions, how it looks, and how it works (Van Gerpen et al., 2004). The terms "initial boiling point, IBP" and "final boiling point, FBP" are used in the context of distillation to describe the temperature range at which different fractions of a liquid mixture are vaporized and condensed. In the case of distillation of diesel fuel, the initial boiling point refers to the temperature at which the first vapor fraction is generated during the distillation process, while the final boiling point represents the temperature at which the last vapor fraction is condensed (Van Gerpen et al., 2004).

There is just one boiling point for pure substances. However, there are a variety of boiling points for the various fractions in liquid fuel, which contain a mixture of hydrocarbons.

A distillation test can be used to find such boiling points. The performance, storage, and safety of the fuels are significantly impacted by these temperature ranges. One of the common test procedures for distilling petroleum products that can be used to gauge boiling temperature ranges is ASTM D86 (Van Gerpen et al., 2004).

The distillation range should generally be as small as feasible without compromising the fuel's flash point, burning characteristics, heat content, or viscosity. Poor starting of the engine may occur if the temperature at which 10 % of the fuel is recovered is too high. An excessive boiling range of 10 to 50 % of the volume recovered may lengthen the warm-up period. It's preferable to have a low temperature at which 50 % of the fuel is recovered to reduce smoke and odor. Lower temperatures at which 90 % of the fuel is recovered and a lower final boiling temperature tend to ensure low carbon residuals and minimal crankcase dilution. Extremely low temperatures at which 50 % of the fuel is recovered result into a low viscosity and a low heat content per unit volume. Therefore, for the higher-speed diesel engines, a temperature in the range of 232 °C to 280 °C is preferred (George et al., 2003). Moses (2014) determined the temperatures at which 50 % of the fuel was recovered as 232.5 °C and 235.6 °C for the distillation tests performed using liquid fuel made from a blend of LDPE and HDPE waste plastics.

2.4.5 Cetane number

Cetane number is a direct measure of the ignition quality of diesel fuel. It represents the percentage of cetane, a pure hydrocarbon compound, in a mixture with another hydrocarbon that exhibits similar ignition characteristics as the fuel being tested. A higher cetane number indicates better ignition quality, meaning the fuel ignites more readily and efficiently. Cetane number describes the rate at which diesel fuel must be compressed and burnt in order to ignite (George et al., 2003). Engine problems might arise when the cetane number is low or high. With greater compression brought on by premature ignition due to high cetane number, engine output is decreased. On the other side, a lower cetane number may result in diesel knock, which is a sudden increase in pressure brought by a mixture's quick combustion after a prolonged ignition in which a sizable portion of the charge enters the cylinder (Macharia, 2018).

Lower cetane number is frequently indicated by higher exhaust gas temperatures and

incomplete combustion, among other things. The standard test procedure for the ignition quality of diesel fuels by the cetane method, ASTM D 613, can be used to determine the cetane number. However, it can be calculated approximately using the cetane index using two test techniques, ASTM D 976 and ASTM D 4737 (George et al., 2003). The cetane index is an estimated value derived from the fuel's density and distillation properties. It is a calculated parameter rather than a direct measurement. The cetane index correlates with the cetane number but does not provide an exact match. It is commonly used when the actual cetane number cannot be directly determined (George et al., 2003). ASTM D976 gives the following equation for Calculated Cetane Index (CCI)

$$CCI = 454.74 - 1641.416D + 774.74D^2 - 0.554T_{50} + 97.803(T_{50})^2 \quad (2.1)$$

where; D is the density at 15 °C in g cm^{-3}, determined using ASTMD 1298, T is the temperature in °C at which 50 % volume of the fuel is recovered during distillation, determined using ASTM D86.

The minimum required value for diesel fuel standards is 48.0 (ASTM, 2003) and it indicates the readiness of such fuel to ignite by itself in the engine cylinder (Van Gerpen et al., 2004)

2.4.6 Ash Content

Ash, defined as the incombustible fraction of a fuel, can take the form of particulate (dirt and/or rust) or oil-based or substances soluble in water, and must be kept to a minimum. Fuels containing these chemicals may generate abrasive ash, which can cause premature piston and cylinder wear (George et al., 2003). Coking on injector nozzles and severe effects on particulate filters are both caused by fuel ash (Van Gerpen et al., 2004). As the percentage of ash in fuels rises, the fuels' ability to generate heat is diminished due to the presence of these compounds. Ash levels in diesel fuel are capped at 0.01 % (m/m) when measured in line with ASTM D482. According to Khan et al. (2016), the ash content in HDPE fuel was 0.036 % (m/m), which is significantly higher than the required minimum value of 0.01 % (m/m) for diesel fuel. Such fuels may undergo incomplete combustion.

2.4.7 Calorific value

Calorific value is the potential energy output of any given fuel when it is burned. The amount of energy contained in fuel is proportional to the number of hydrocarbons it contains. The calorific value of a fuel is a crucial characteristic that indicates the amount of energy stored in the fuel's chemical bonds and it also controls how well a compression ignition engine retains heat (Macharia, 2018).

Plastic materials have a high calorific value greater than 40 MJ/kg (Singhabhandhu and Tezuka, 2010) since they contain a lot of carbon and hydrogen, and little ash (Macharia, 2018). However, based on the thermal decomposition and the type of plastic material, the energy content of fuel generated from plastic could be greater or lower than that of petroleum. Plastic has a high calorific value, which suggests that liquid fuel made from plastics can be used in substitution for fossil fuels.

Table 2.1: Diesel fuel quality requirements (UNBS, 2019)

Property	**Limits**		**Test methods**
	Minimum	**Maximum**	
Cetane number	51.0	-	ISO 5165
Cetane index	48	-	ASTM D976
Density at 15 °C /g cm^{-3}	0.820	0.870	ASTM D1298
Copper strip corrosion for 3 h at 50 °C/rating	Class 1	Class 1	ASTM D130
Kinematic viscosity at 40 °C/mm^2/s	2.0	5.3	ASTM D445
Ash content % (m/m)	-	0.01	ASTM D482
Distillation			ASTM D86
(a) IBP/^oC	-	-	
(b) % recovered at 250^oC	-	65	
(c) % recovered at 350^oC	85	-	
(d) 95% recovery/^oC	-	360	
(e) FBP/^oC	-	400	

2.5 Performance of Internal Combustion engines

The performance of an engine is a good predictor of how well it will fulfill the tasks it has been given. It demonstrates how the chemical energy in the fuel is transformed into use-able mechanical energy (Macharia, 2018). The primary objective in the design and development of IC engines is to lower production costs and boost efficiency and output power. Therefore engine tests and measurement of relevant parameters that reflect

engine performance must be evaluated (Heywood, 2018). The significant performance parameters of IC engines are discussed in the following subsections.

2.5.1 Brake Power

The power available at an engine's output shaft is called its brake power (Ferrari et al., 2022). It is the power that can be positively used against the braking force of the application for which the engine is being used. Brake power measurement involves the determination of torque and angular speed of the engine output shaft using a dynamometer and a speed tachometer. A dynamometer imposes variable loading conditions on the engine under test, across a range of engine speeds and duration, thereby enabling accurate measurement of torque and power output of the engine (Atkins, 2009). Figure 2.3 shows the basic principle of a dynamometer.

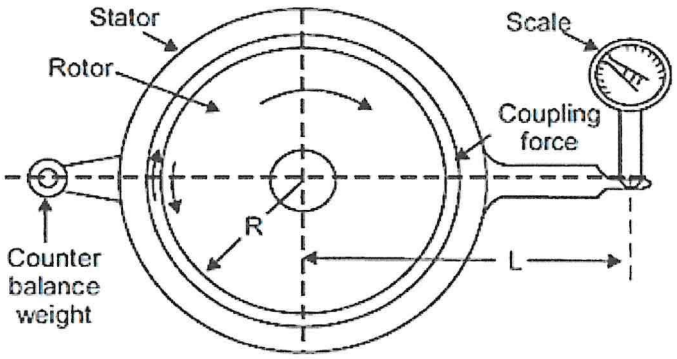

Figure 2.4: Principle of a dynamometer (Atkins, 2009)

Through mechanical, hydraulic, or electromagnetic means, the engine under test drives a rotor that connects to a stator. As the shaft rotates, the rotor periphery moves through a distance of $2\pi RF$ against the force, F, exerted. hence the work done per revolution is calculated from equation 2.2

$$W = 2\pi RF \tag{2.2}$$

The external moment or torque, $T = S \times L$, where S is the weight of the load recorded from the scale and L is the arm length. This moment balances the turning moment $R \times F$, implying that;

$$S \times L = R \times F \tag{2.3}$$

Therefore,

$$\text{work done per revolution} = 2\pi SL \tag{2.4}$$

$$\text{work done per minute} = 2\pi SLN \tag{2.5}$$

where N is angular speed. Hence Brake power can be calculated using equation

$$\text{Brake Power (BP)} = 2\pi TN \tag{2.6}$$

2.5.2 Thermal Efficiency

The amount of energy that reaches the flywheel or the dynamometer compared to how much theoretically could be released is a function of three efficiencies: thermal, mechanical and volumetric efficiency. Thermal efficiency is the ratio of work generated in a cycle to fuel energy provided per cycle that can be released in combustion(Atkins, 2009). It can be based on indicated power or brake power. Indicated power is the power output produced by the combustion process within the engine cylinder. It represents the power developed by the combustion of fuel and air mixture in the combustion chamber. Engine thermal can accordingly be specified as;

$$\text{Indicated thermal efficiency} = \frac{\text{IP}}{\dot{m}_f \times c} \tag{2.7}$$

$$\text{Brake Thermal Efficiency (BTE)} = \frac{\text{BP}}{\dot{m}_f \times c} \tag{2.8}$$

$\dot{m}_f$ is the rate of fuel consumed, Indicated Power (IP) is indicated power, BP is brake power, and c is the calorific value of the fuel. When the load on the engine goes up, the engine's thermal efficiency goes up until it reaches its peak. After that, it starts to go down.

2.5.3 Specific Fuel Consumption

This engine parameter provides a measure of how efficiently an engine is using fuel supplied to produce work (Atkins, 2009). The amount of fuel an engine needs to use to make one unit of power is called its Specific Fuel Consumption (SFC). It generally indicates the amount of fuel an engine can consume in terms of mass or volume (Atkins, 2009). It is a measure of how efficiently an internal combustion engine consumes fuel.

The amount of fuel an engine consumes over a certain period of time can be measured in terms of volume or mass. From the brake power and the indicated power, Brake Specific Fuel Consumption (BSFC) and the Indicated Specific Fuel Consumption (ISFC) can be determined using equations 2.9 and 2.10 respectively.

$$\text{BSFC} = \frac{\dot{m}_f}{\text{BP}} \tag{2.9}$$

and

$$\text{ISFC} = \frac{\dot{m}_f}{\text{IP}} \tag{2.10}$$

Specific fuel consumption varies with engine size, operation load, and engine design. Brake-specific fuel consumption generally decreases with engine size because less heat is lost due to the higher volume-to-surface area ratio of the combustion chamber in large engines and also large engines operate at lower speeds which reduce friction losses (Atkins, 2009). Brake-specific fuel consumption decreases as engine speed increases, reaches a minimum, and then increases at high speeds as shown in Figure 2.4.

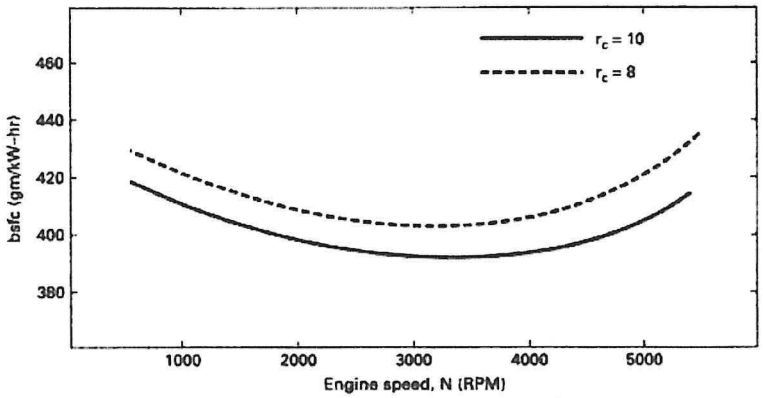

Figure 2.5: Brake specific consumption vs engine speed (Atkins, 2009)

Fuel consumption increases at high speeds because of greater friction losses and at low engine speed, the longer time per cycle allows more heat loss, and more fuel consumption.

Chapter 3

Methodology of the Study

3.1 Introduction

This chapter explains the methodology that was used to carry out the study. It gives an overview of the process that was used to turn different kinds of plastics into liquid fuel using the fabricated pyrolysis system. It also covers standard tests for assessing the characteristics of diesel and liquid fuel from plastics. In addition to that, the chapter lays out the steps that must be taken in order to evaluate the performance of the engine.

3.2 Research Design

Both quantitative and experimental methods were used in this investigation. Standard Test Methods for automotive diesel standards were used to analyze the density, kinematic viscosity, ash content, cetane index, distillation properties, copper strip corrosion, and calorific value of standard diesel and the fuel samples produced via pyrolysis from HDPE and PP plastic. Engine efficiency was evaluated while using this fuel and standard diesel.

3.3 Fabrication of the Pyrolysis System

3.3.1 Pyrolysis reactor design and fabrication

A mild steel gas cylinder was used to fabricate a batch pyrolysis reactor with the following dimensions: 0.3 cm thick, inner diameter 29.7 cm, outer diameter 30.0 cm, and height 60.0 cm. The top of the cylinder was drilled with a 5.0 cm hole as the plastic loading

point. Two holes of 2.0 cm diameter were also drilled on the cylinder as in Figure 3.1. A k-type thermocouple sensor with a temperature range of -50 to 1350 °C was attached to one of the 2 cm holes and the other was connected to the outlet pipe.

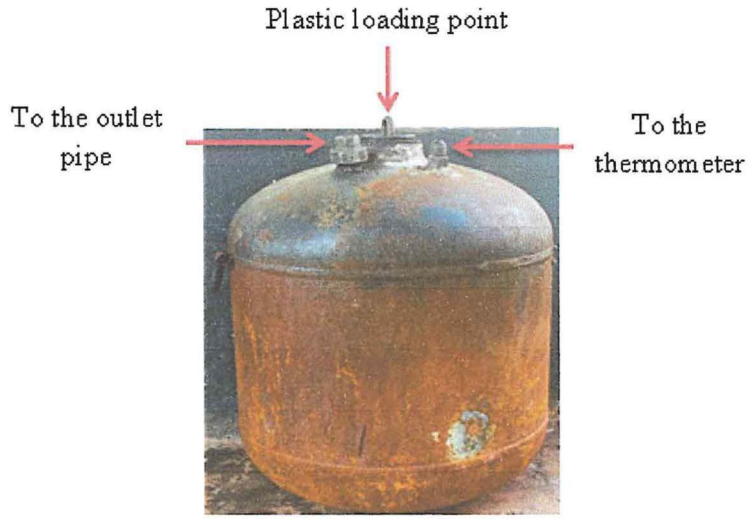

Figure 3.1: Fabricated pyrolysis reactor

3.3.2 Condenser design and fabrication

A mild steel pipe (0.3 cm thick, 10 cm internal diameter, and 175 cm in length) was used to make a condenser in the shape of a cylinder. Circular metal parts were used to enclose the ends, and holes of 2 cm in diameter were made in the circular metal parts for the outlet pipe of length 180 cm to pass through. The pipe was drilled with two holes one at each end, measuring 2 cm in diameter at the top and another at the bottom, to allow cold water in and warm water out respectively (Figure 3.2).

Figure 3.2: Fabricated condenser

3.3.3 Pyrolysis system

The reactor and condenser were then welded using electricity and welding sticks, tightly sealed using liquid petroleum gas to avoid any leakages. A heating stove was designed such that at least three-quarters of the reactor is insulated during the production process to minimize heat loss. The pyrolysis system was completed by placing the reactor in the heating stove, connecting the condenser and the vapour outlet pipe through the condenser using union connectors, to the collection unit as shown in Figure 3.3. The condenser was coupled to an overhead plastic water tank with enough water to enable water flow by gravity. The tank was supported by a custom-made platform.

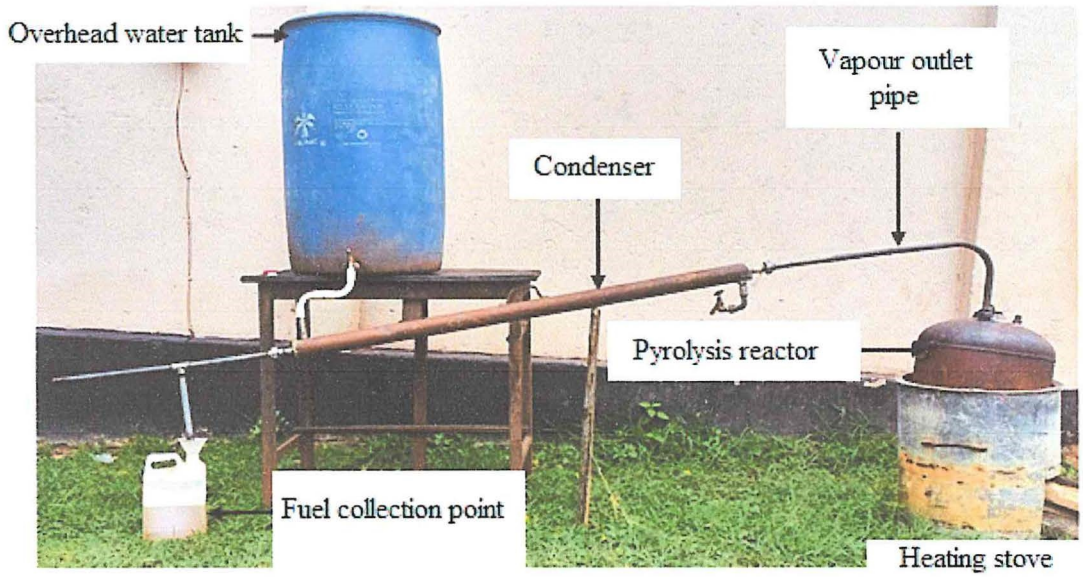

Figure 3.3: Fabricated pyrolysis system for production of liquid fuel

3.4 Sample Collection and preparation

Plastics were collected, manually sorted, and grouped into various types. The sorted HDPE and PP plastics were then cleaned with water and soap to get rid of any dirt that would interfere with the melting process. Using scissors, the clean, dried plastics were cut into smaller pieces of about 2 cm by 2 cm to ensure a larger contact surface area with the reactor. Based on the capacity of the designed reactor, 9 kg of each HDPE and PP plastics were measured using a weighing scale, stored in buckets, and marked as HDPE and PP, respectively.

3.5 Production of Liquid Fuel from Plastics

The HDPE and PP plastics that had been processed were each in turn fed into the reactor using the 5 cm hole which was then tightly sealed. Using firewood, the plastics were heated until they melted and evaporated. The resulting vapour was condensed in the condenser unit at a temperature equivalent to the surrounding air. A thermocouple thermometer and a stop clock were used to measure the pyrolysis temperature and residence time respectively. The liquid byproduct discharged from the condenser was collected in a container located at the end of the outflow pipe. The volume of the liquid product obtained from each type of plastic was measured using a measuring cylinder, recorded, and labeled as High-Density Polyethylene Liquid Fuel (HDPELF) and Polypropylene Liquid Fuel (PPLF). The mass of the liquid fuel was then obtained using the measured density of the fuel. After 8 to 10 hours, the residue was removed from the reactor, weighed using an electronic balance, and its mass was recorded. The gas yield was determined by mass balance of the plastics used in the reactor using equation 3.1.

$$\text{Mass of Gas} = \text{Mass of plastics} - (\text{Mass of liquid fuel} + \text{Mass of solid residue}) \quad (3.1)$$

The percentage product yield was then calculated using equations 3.2, 3.3, and 3.4.

$$\text{Percentage liquid product} = \frac{\text{mass of liquid product}}{\text{mass of HDPE plastics}} \times 100\% \quad (3.2)$$

$$\text{Percentage solid residue} = \frac{\text{mass of solid product}}{\text{mass of HDPE plastics}} \times 100\% \quad (3.3)$$

$$\text{Percentage gas product} = \frac{\text{mass of gas product}}{\text{mass of HDPE plastics}} \times 100\% \quad (3.4)$$

Before analysis of the liquid fuel obtained, one litre of HDPELF was mixed with one litre of water in a two-litre measuring cylinder, shaken well for about 5 minutes, and allowed to settle for about 7 - 8 hours to further remove the dirt and other components in the fuel. After some time, water and other particles settled at the bottom, while the necessary fuel was recovered from the top, by gently pouring it into another two-litre measuring cylinder. The PH value of each sample was determined using a universal indicator solution and colour charts in order to monitor the potential corrosiveness of the fuel towards plastics or other materials that may come into contact with the fuel during storage, transportation,

or use. The liquid fuel obtained was then stored and ready for analysis.

3.6 Measurement of the Properties of Liquid Fuel from Plastics

The physical parameters were determined by conducting analyses on the samples of HD-PELF and PPLF. For comparison and calculation of engine parameters, the properties of standard diesel were also determined, as discussed in the following subsections.

3.6.1 Density

ASTM D1298 was used to measure the density of diesel and fuel from plastics (Nadkarni and Nadkarni, 2007). A single transparent 100 ml glass measuring cylinder was used. A volume of 100 ml of the fuel sample was measured, put in the cylinder and then placed in a refrigerator for some time until its temperature was below 15 ^{o}C, to cater for the heat that can be gained during transfer from the refrigerator. The cylinder and its content were then removed from the refrigerator. A hydrometer and a thermometer were lowered into the diesel sample. The hydrometer scale was read when the temperature of the diesel sample was 15 ^{o}C for quality control as indicated in Table 2.1.

3.6.2 Kinematic Viscosity

Cannon Fenske viscometer tube labeled Koehler size 100 was used to measure the fuel's kinematic viscosity in accordance with the ASTM D445 standard test method for kinematic viscosity of transparent and opaque liquids (ASTM, 2003). To avoid contamination of the fuel samples, dilute nitric acid and distilled water were used to clean the viscometer prior to the test. After ensuring that the viscometer tube was dry, a dropper was used to introduce 6 ml of the fuel sample into tube "C" (Figure 3.4 (a)). The viscometer tube was then clamped in its holder and mounted in a viscometer bath as shown in Figure 3.4 (b), set at 40 ^{o}C, a standardized temperature for viscosity testing in the petroleum industry. The set-up was left for 20 minutes at 40 ^{o}C. Suction was applied to tube "D" using a rubber sucker until the fuel sample just raised beyond the line marked "A". Upon reaching line A, the start button on the stopwatch was pressed, and it was stopped when the fuel sample just crossed line B. The flow time, t, was measured and recorded. The kinematic

viscosity of the fuel sample was then calculated using equation 3.5 (ASTM, 2003).

$$\text{Kinematic viscosity} = c \times t \tag{3.5}$$

where c is the vicometer constant.

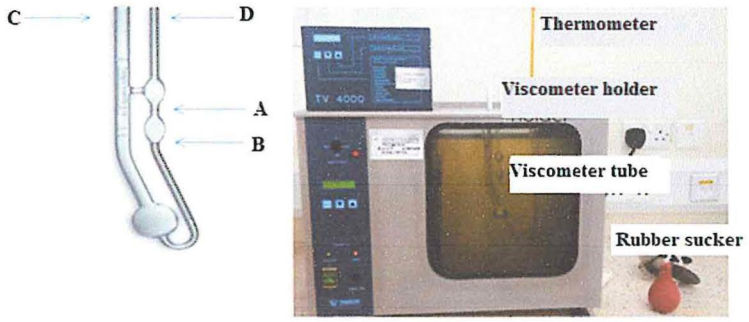

Figure 3.4: (a) Cannon Fenske viscometer tube, (b) Tamson viscometer bath

3.6.3 Ash content

Ash is the incombustible constituent of any fuel that exists as a solid, oil, or materials soluble in water. These materials should be in small amounts because they affect the calorific value of fuels. The fuel's heat value decreases as the ash content increases.

A cleaned, dried crucible was weighed using an electronic balance, and its mass, m_1 noted. A volume of 6 ml of the fuel sample was carefully introduced in the crucible and the mass, m_2 of the crucible and its constituents were noted. The sample in the crucible was ignited and allowed to burn until only ash and carbon remained. Using a muffle furnace, the crucible and its constituents were heated at 775 °C for four hours according to ASTM D482 to convert the entire carbonaceous residue to ash (Nadkarni and Nadkarni, 2007). The crucible was then removed, left to cool, weighed, and its mass, m_3 noted. The ash content of the fuel sample was then obtained using equation 3.4;

$$\text{Ash content} = \frac{m_3 - m_1}{m_2 - m_1} \times 100\% \tag{3.6}$$

The procedures were repeated three times using standard diesel and plastics-derived fuel, from which the mean and standard error values were calculated using descriptive statistics

in MS Excel.

3.6.4 Calorific value

The higher heating values of the standard diesel, HDPELF, and PPLF samples were measured using an internal program in the IKA C2000 digital bomb calorimeter. Three samples were extracted from each fuel sample, each weighing 1.02 g. A sample was then placed in the bomb calorimeter vessel. It was subjected to complete combustion in an adiabatic environment which is internally stabilized by computer software, heaters, and circulating water in the calorimeter. The calorific value was then calculated from the measured increase in temperature in the adiabatic system by the IKA C2000 digital bomb calorimeter software and displayed on its screen. This value was recorded and the procedure was repeated using the other two standard diesel samples. The mean and standard deviation was then calculated using descriptive statistics.

3.6.5 Distillation Characteristics

The distillation process was carried out on standard diesel and liquid fuel from HDPE and PP plastic waste in accordance with ASTM D86 test method using the atmospheric distillation unit shown in Figure 3.5 (ASTM, 2003).

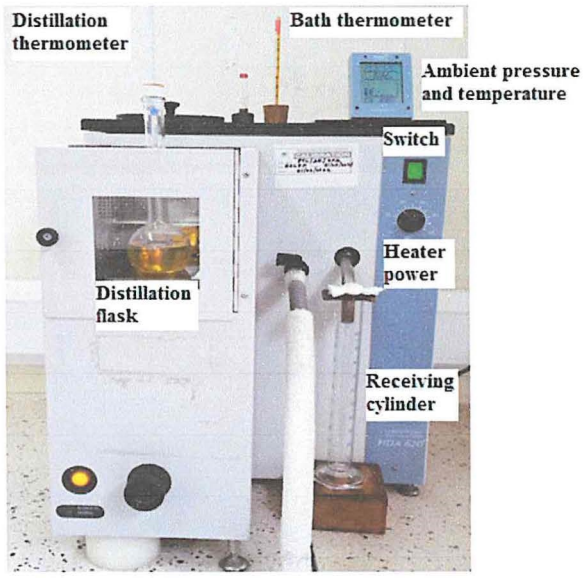

Figure 3.5: Atmospheric Distillation unit

A fuel sample of volume 100 ml was precisely measured and then transferred to a distil-

lation flask. Two clean dry boiling chips were added to the fuel in the distillation flask to calm down the boiling process during the experiment. The distillation flask vapour tube was tightly connected to the condenser and the thermometer was connected to the distillation flask, using a silicon rubber stopper. The distillation flask was adjusted in a vertical position for the vapour tube to extend into the condenser. The receiving cylinder was placed under the lower end of the condenser tube centered in the receiving tube. The distillation unit was then switched on. The observed temperature at which the first drop of the fuel sample is recovered up to the final boiling point, the point at which the temperature begins to decrease was measured. The observed temperature was measured using the thermometer while the volume of the fuel sample recovered was recorded from the receiving cylinder. Distillation curves for the fuel samples were determined to show the quantity of fuel that boils off at a given temperature.

3.6.6 Cetane index

ASTM D 976 standard test method was used to approximate the cetane number of standard diesel, HDPELF and PPLF fuel samples. The temperature corresponding to 50 % volume of fuel recovered for each sample in the distillation process was used to calculate the cetane index using equation 2.1.

3.6.7 Copper strip corrosion

ASTM D130 test method for copper strip corrosion was used to determine the degree of corrosiveness of standard diesel and liquid fuel from HDPE and PP plastics (ASTM, 2003). Three copper strips were polished using silicon carbide to remove all the blemishes and to obtain uniformly stained strips. Each of the polished strips was placed in a test tube and fuel samples added until it was just above each strip. Each test tube was then placed in a test bomb (Figure 3.6 (a)). The test bombs were placed in a constant temperature bath set at 50 ^{o}C to ensure consistency and comparability of results across different experiments. After 3 hours, the copper strips were removed, washed, and compared with ASTM copper corrosion standards shown in Figure 3.6 (b). The corrosiveness of each sample was interpreted accordingly as the appearance of the test strips agreed with one of the strips of the ASTM copper corrosion standards.

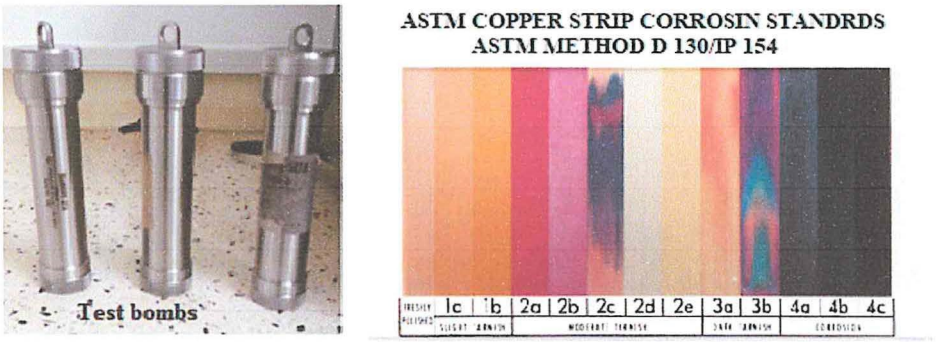

(a) (b)

Figure 3.6: (a) Test bombs, and (b) ASTM copper strip corrosion standards

The extent of corrosion was then graded on a scale from class 1 to class 4.

3.7 Performance Evaluation of Plastic-derived Fuel

3.7.1 Engine set up

The performance of liquid fuel from HDPE and PP plastics was evaluated using 1Z Ruston & Hornsby horizontal single cylinder four stroke water-cooled diesel engine rated 475 rpm, located in the internal combustion room at the Department of Mechanical and production engineering, Kyambogo University. The performance was then compared to standard diesel using the same engine.

3.7.2 Engine test procedure

Four litres of each fuel sample were in turn placed in the engine supply tank connected to a burette using a tap. The tap was opened until the burette was filled. The engine was loaded with 5 kg attached to its dynamometer. Once the engine reached a state of stability that is at a constant speed, the speed of the engine and the duration it took to consume 20 ml of the fuel sample under this load were recorded. This was repeated using 10, 15, 20, 25, 30, and 35 kg loads and the results were noted. The fuel lines were drained before another fuel sample was introduced.

3.7.3 Mass flow rate of the fuel

A burette connected to the fuel supply system was filled with a fuel sample from the main fuel tank. The time, t, taken for the engine to consume 20 ml of the fuel sample was measured using a stopwatch and the fuel mass rate, $\dot{m}_f$, was calculated using equation 3.7 (Atkins, 2009).

$$\dot{m}_f = \frac{\rho \times 20}{t}, \tag{3.7}$$

Where ρ is the density of the liquid fuel sample. This was repeated five times for each fuel sample at different loads to improve the accuracy, understand the variability, and detect systematic errors. The mass flow rate was then recorded.

3.7.4 Brake power

This is the usable power output of an engine, not including the power required to fuel, lubricate, or heat the engine, circulate coolant to the engine, or operate after-treatment devices. It is the power available at the crankshaft. Its measurement involves the determination of brake torque using a dynamometer as well as the angular velocity of the engine's output shaft. This was calculated using equation 3.8 (Atkins, 2009).

$$\text{BP} = \frac{2\pi(\text{V} \times \text{T})}{60000}\text{kW}, \tag{3.8}$$

where V is the angular speed of the engine and T is the brake torque.
However, brake torque is calculated from equation 3.9.

$$\text{T} = \text{L} \times \text{R}, \tag{3.9}$$

where R is the radius of the flywheel.

3.7.5 Brake specific fuel consumption, BSFC

This is the amount of fuel consumed by an engine for each unit of brake power developed per hour. It is a clear indication of the efficiency with which the engine develops power from a given fuel. Brake-specific fuel consumption was calculated using equation 3.10 (Atkins, 2009).

$$\text{BSFC} = \frac{\dot{m}_f}{\text{BP}}, \tag{3.10}$$

3.7.6 Brake thermal efficiency

Brake thermal efficiency is the true indication of the efficiency with which the chemical energy of the fuel is converted into mechanical work. Brake thermal efficiency was determined using the engine's brake power and fuel power using equation 3.11 (Atkins, 2009).

$$\text{Brake thermal efficiency} = \frac{\text{BP}}{\text{Fuel power}}, \tag{3.11}$$

Where Fuel power is the product of fuel mass flow rate and calorific value of the fuel sample.

Chapter 4

Results and Discussion

4.1 Introduction

This chapter illustrates and discusses the results of the study in line with the objectives of the study. It outlines the products of plastic pyrolysis process using the fabricated pyrolysis system. The chapter discusses the fuel properties of standard diesel and liquid fuel from plastics as determined using standard test methods during laboratory tests. Finally, the chapter tabulates and discusses the results from engine performance tests using standard diesel and liquid fuel from plastic.

4.2 Production of liquid fuel from plastics

During the production process, pyrolysis temperature, and residence time, the duration for plastics to be heated to the time when no more liquid product is obtained were observed and recorded. Further conversions are more likely when there is a longer residence time, and hence enhances the product yield (Marcilla et al., 2007). The percentage product yield was also determined after pyrolysis of each plastic type as discussed in the following subsections.

4.2.1 Pyrolysis temperature and residence time

Pyrolysis temperature and residence time were observed to find out the range of temperature that can give the maximum liquid product and the duration for this to be attained. During the production process, the pyrolysis temperature for PP and HDPE plastics was

observed in the range of 34 °C to 410 °C and 27 °C to 420 °C for 3 hours, and 3 hours 13 minutes respectively as shown in Table A.1 and Table A.2 (APPENDIX A). From these tables, Figure 4.2 was obtained.

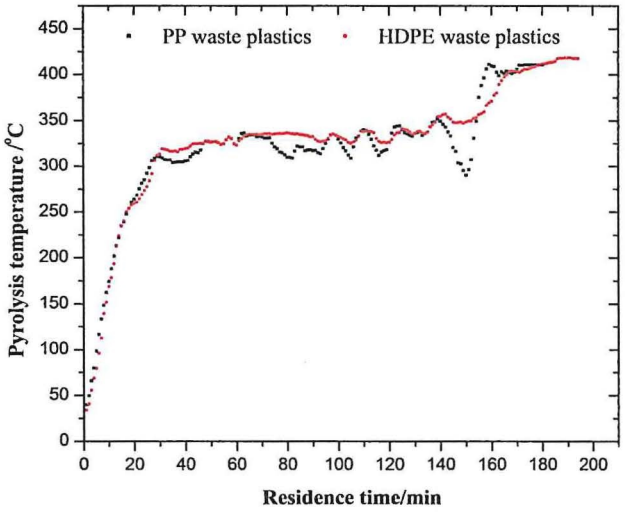

Figure 4.1: Variation of Pyrolysis Temperature with Residence Time

From Figure 4.1, PP plastic was heated from 34 °C by increasing the heat at an approximate rate of 12.59 °C/min and after 17 minutes, at 247 °C, the first liquid drop was obtained. In order to condense more vapors, the heating rate was reduced to approximately 0.738 °C/min by removing some firewood from the heating stove and the process was observed for 1 hour and 50 minutes. This is when the maximum liquid yield was achieved from PP plastics in a temperature range of 300 °C to 350 °C. The rate was then increased to approximately 1.41 °C/min for further 53 minutes up to 410 °C where no more liquid drops were collected.

High-density polyethylene plastics were heated from 27 °C by adding more fire at an approximate rate of 10.77 °C/min and after 22 minutes, at 265 °C, the first liquid drop was obtained. In order to condense more vapors, the heating rate was reduced to approximately 0.61 °C/min by removing some firewood from the heating stove and the process was observed for 1 hour and 53 minutes up to 350 °C and this is when the maximum liquid yield was achieved from HDPE plastics. The temperatures between 300 °C and 350 °C were fairly controlled (by adding and/or removing firewood) for a longer time in

order to condense most of the vapour into liquid fuel.

4.2.2 Percentage product yield

After 3 hours of heating PP plastics, 79.8 wt% liquid fuel, and 2.6 wt% solid residue were collected with 17.6 wt% estimated as the gaseous product. High-density polyethylene plastics were heated for 3 hours and 13 minutes and after this time, 81.2 wt% of liquid fuel and 5.8 wt% of solid residue had been collected with 13.0 wt% estimated as the gaseous product as shown in Figure 4.2.

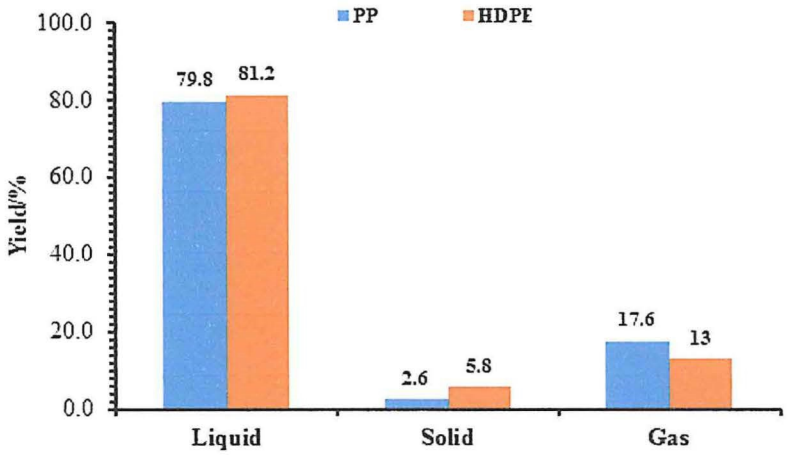

Figure 4.2: Product yield from HDPE and PP plastics

A production yield of up to 83 wt. % of diesel oil was recovered from Polypropylene waste plastics using a fixed bed reactor in vacuum conditions at 600 °C to 650 °C (Thahir et al., 2019). This range of liquid percentage yield is higher than the 79.8 wt% achieved in the current study. The variation may be attributed to the vacuum conditions which may have not been accurately attained in the current study, and the loss of more vapour not condensed. In a study by Olufemi and Olagboye (2017), LDPE, HDPE, and PP waste plastics and their mixture were pyrolyzed at temperatures between 170 °C and 300 °C under atmospheric conditions to generate liquid fuel. The individual product percentage yield attained was reported as; 91.981 wt% liquid, 2.073 wt% gas, and 5.944 wt% solid residual from PP plastics, 89.354 wt% liquid, 5.345 wt% gas, and 5.299 wt% solid residual from HDPE waste plastics. The liquid percentage yield from both plastic types is higher than the 79.8 wt% and 81.2 wt% yield obtained in this study. In this study, the estimated percentage yield of gas is higher than that of Olufemi and Olagboye (2017),

because more vapour was not condensed leading to a decrease in the liquid product. Probably, the high yield of liquid and solid residue obtained from HDPE plastics is attributed to its high density compared to PP plastics whose percentage yield was low.

4.3 Properties of standard diesel and fuel from plastics

4.3.1 Density

The density of standard diesel, HDPELF and PPLF obtained in this study were 0.830 ± 0.001, 0.790 ± 0.003 and 0.788 ± 0.001 g cm^{-3} at 15 °C and 0.825 ± 0.001, 0.786 ± 0.003 and 0.784 ± 0.001 g cm^{-3} at at 20 °C. A similar range of density values was obtained by Quesada et al., 2019; Owusu et al., 2018; Chandrasekaran, 2019; Moses, 2014; Kyaw, 2015; Mustafa, 2019; Khan et al., 2016 and Bhat, 2016.

ASTM D1298, ISO 3675, and Uganda National Bureau of Standards (UNBS) consider a range of density of standard diesel as 0.817 – 0.867 g cm^{-3} at 20 °C and 0.820 – 0.870 g cm^{-3} at 15 °C. The density values obtained in this study are close to the density of standard diesel fuel at these temperatures. Therefore, HDPELF and PPLF can supplement standard diesel fuel.

The density of fuel has an effect on the amount of power produced by an engine, as well as its emissions and the amount of fuel it consumes (George et al., 2003). Since the density of HDPELF and PPLF is lower than the density of conventional diesel, engine power output is expected to be lower than when it is run on standard diesel fuel, and fuel consumption is expected to increase.

4.3.2 Ash Content

From Figure 4.3, standard diesel fuel, HDPELF, and PPLF had a percentage ash content of 0.02, 0.03, and 0.02 % (m/m) respectively. Standard diesel and PPLF samples had an equal amount of ash content compared to HDPELF. Considering the error bounds, the ash content of standard diesel agrees with the specified maximum value of 0.01 % (m/m) for diesel fuel as per UNBS while that of HDPELF and PPLF is slightly higher than the accepted value of $\leq 0.01\%$.

Khan et al., (2016) obtained liquid fuel from HDPE plastic waste whose ash content was 0.036 % (m/m) comparatively higher than the 0.03 obtained in the current study. The discrepancy may be due to the cleaning process used by Khan et al., (2016) which may have left more dirt in the plastics prior to the production process. This implies that the fuel obtained from plastics in the current study can undergo better combustion in CI engines. This is because High ash content can adversely affect the combustion process by depositing on critical engine components, such as fuel injectors, combustion chambers, and exhaust systems. These deposits can hinder fuel atomization, disrupt airflow, and impede heat transfer, leading to reduced combustion efficiency, increased fuel consumption, and decreased engine performance (George et al., 2003). Ash deposits can accumulate on surfaces, causing abrasive or corrosive effects, leading to accelerated wear and potential damage to fuel injectors, piston rings, valves, and exhaust systems. Over time, excessive ash buildup can lead to decreased engine performance, increased maintenance costs, and shortened engine lifespan Wright and Purday (1950).

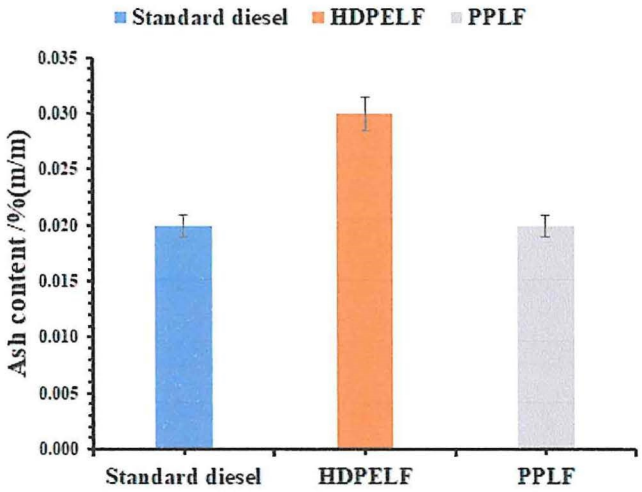

Figure 4.3: Ash content of standard diesel and fuel from plastics

4.3.3 Distillation Characteristics

The observed temperature at which the volume of fuel sample was recovered, was recorded as shown in Table B.1 (APPENDIX B) from which distillation curves were obtained to show the quantity of fuel that boils off at a given temperature as shown in Figure 4.4.

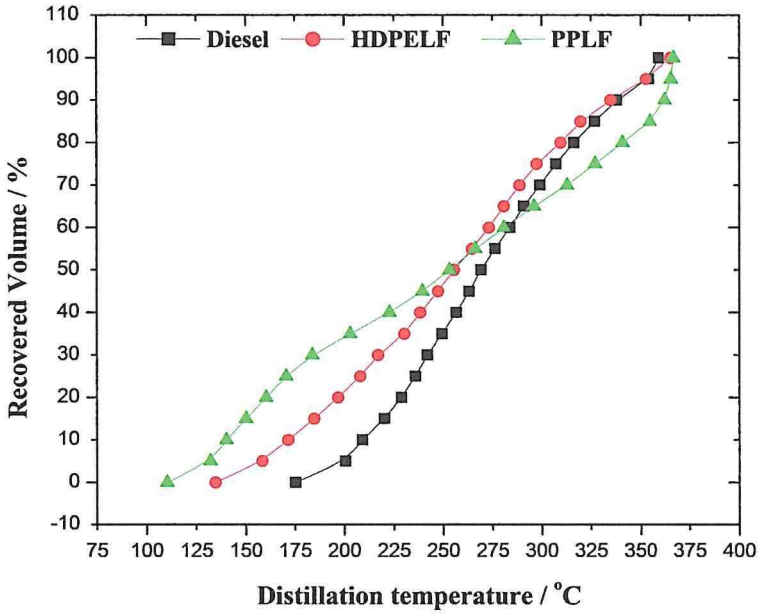

Figure 4.4: Distillation Characteristics of Diesel, HDPELF and PPLF

There is more deviation at the beginning and less deviation at center and at the end of the distillation of the three fuel samples. The three fuel samples closely agree at the 50 % recovered volume. Liquid fuel from plastics was more volatile than standard diesel between 0 % and 50 % recovered volume. This is because Plastics are made up of various polymers and additives, which can result in a complex mixture of hydrocarbon compounds when processed into fuel. These hydrocarbons can have different boiling points and volatility characteristics compared to conventional diesel fuel. The presence of lighter hydrocarbons or compounds with lower boiling points in plastic-derived fuels can contribute to their increased volatility. This reduces the power output of the engine through vapour lock (George et al., 2003).

The volume of fuel sample recovered at 250 °C was observed as 41.0, 51.0, and 52 % (v/v) for standard diesel, HDPELF, and PPLF respectively. These values are within the standard required value of less or equal to 65.0 % (v/v). In the same way, the volumes recovered at 350 °C were observed as 96.0, 95.0, and 87.0 % (v/v) for standard diesel, HDPELF, and PPLF respectively. These values are within the standard value of greater than 85.0 % (v/v) at 350 °C (UNBS, 2019).

It is observed that the Initial Boiling Point (IBP) and Final Boiling Point (FBP) of HDPELF were in the range of 135 °C and 365 °C respectively, while the boiling range of PPLF was 110 °C – 366 °C. The difference in the boiling ranges is attributed to plastics containing different additives like plasticizers, stabilizers, or flame retardants, which impact the volatility of the resulting fuel. Some of these additives may have low boiling points and easily vaporize, contributing to the overall volatility of the plastic-derived fuel. This boiling temperature range is comparable to the ranges obtained by Owusu et al. (2018) for fuel obtained from HDPE and PP plastics. According to Kumar et al. (2016), the observed temperature range shows that there are different fuel fractions like diesel, petrol, and kerosene that can further be separated from HDPELF and PPLF.

4.3.4 Cetane Index

The average temperatures at which 50 % of the distillate was recovered (Table B.1, APPENDIX B) were used together with the density at 15 °C (Table 4.1) of each fuel sample to calculate the cetane index of each fuel sample using equation 2.1. The results obtained are presented in Figure 4.5.

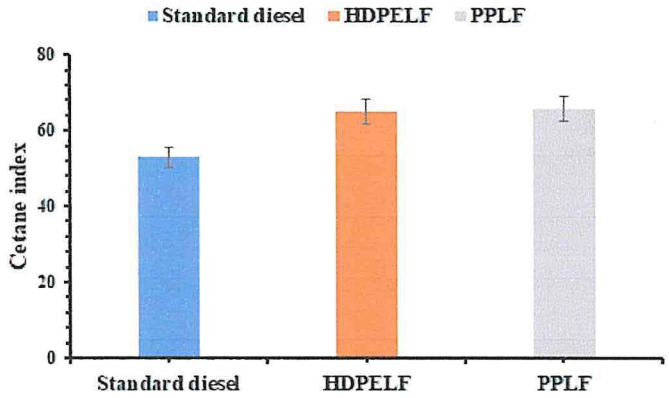

Figure 4.5: Cetane index of standard diesel and fuel form plastics

From Figure 4.5, the calculated cetane index values were 53, 65, and 66 for standard diesel, HDPELF, and PPLF respectively. Cetane index values were above 48 as per diesel fuel specifications indicated in Table 2.1. The range of 65 and 66 of fuel samples from plastics indicates better ignition quality, meaning the fuel will ignite more readily and efficiently when subjected to high temperatures and pressure within the engine's combustion chamber. This results into good combustion quality hence achieving optimal engine

performance, including smooth operation, reliable ignition, and efficient fuel consumption while using such fuels (Van Gerpen et al., 2004). The results in this study are slightly greater than 62 and 64 obtained by Miskolczi et al. (2009) and Moses (2014). Lower cetane indices of 46 and 63 for waste plastic fuel from HDPE and PP were obtained by Owusu et al. (2018).

4.3.5 Kinematic viscosity

Figure 4.6 shows the average values of the kinematic viscosity of standard diesel, HDPELF and PPLF found to be, 2.71 ± 0.04, 2.00 ± 0.04 and 2.04 ± 0.02 cSt respectively. These values were higher than 1.44 cSt and 1.98 cSt from HDPE plastic waste, obtained by Khan et al., (2016) and Macharia, (2018) respectively, but lower than 2.373 cSt and 2.115 cSt of waste plastic oil obtained by Owusu, (2018), from HDPE and PP plastic waste respectively. The viscosity of standard diesel was higher than that of HDPELF and PPLF by about 25.9 % at a standard temperature of 40 ^{o}C. However, the kinematic viscosity of HDPELF and PPLF was within the acceptable range of values for automotive diesel fuel of 2.0 – 5.3 cSt as shown in Table 2.1 (UNBS 2019).

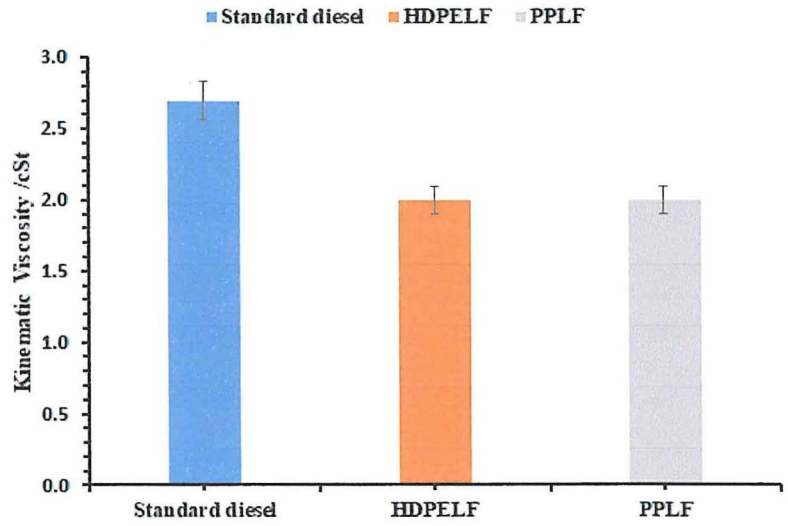

Figure 4.6: Kinematic viscosity of standard diesel and liquid fuel from plastics

4.3.6 Calorific value

The calorific value of standard diesel, HDPELF and PPLF was measured as 47.59 ± 0.49, 48.65 ± 0.13 and 48.52 ± 0.00 MJkg^{-1} as shown in Figure 4.7.

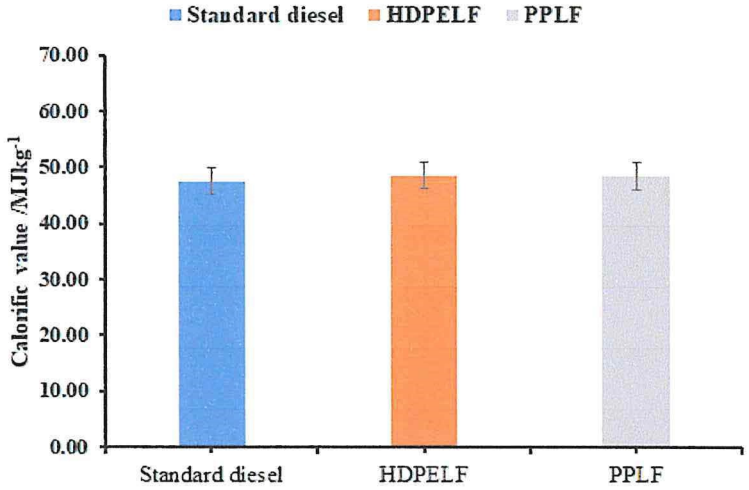

Figure 4.7: Calorific values of diesel and fuel from plastics

It is observed that the calorific value of standard diesel fuel is lower than that of liquid fuel from HDPE and PP waste plastics. This means that the amount of heat energy that is released by HDPELF and PPLF after combustion is greater than that of standard diesel by 2.2 % and 1.9 % respectively. Therefore, HDPELF and PPLF can be a better supplement to standard diesel in terms of energy production in combustion engines.

4.3.7 Copper strip corrosion

The corrosiveness of PPLF was found to be class 1a similar to that obtained for standard diesel. The copper strip showed no visible signs of corrosion, indicating that the tested sample is non-corrosive towards copper. Liquid fuel obtained from HDPE had a corrosion level of class 3a which indicates moderate corrosion on the copper strip, typically characterized by distinct tarnish and discoloration. However, there is no complete loss of copper. Therefore the corrosive effect of liquid fuel from plastics on copper-based materials, as copper corrosion can lead to equipment degradation, leaks, and other operational issues, is just like standard diesel.

A summary of the properties of standard diesel and plastic-derived fuel, as discussed above is presented in Table B.2 (APPENDIX B).

4.4 Performance Evaluation of Liquid Fuel

The performance of standard diesel and liquid fuel from plastics was assessed based on braking power, brake thermal efficiency, and brake-specific fuel consumption in a CI engine. The engine parameters were determined based on the time the engine took to consume 20 ml of the fuel samples.

4.4.1 Fuel consumption time

The time taken to consume 20 ml of each fuel sample with variations in the engine load was recorded as shown in Table C.1 (APPENDIX C) from which a graph of time taken to consume 20 ml of fuel against engine load was obtained as shown in Figure 4.8.

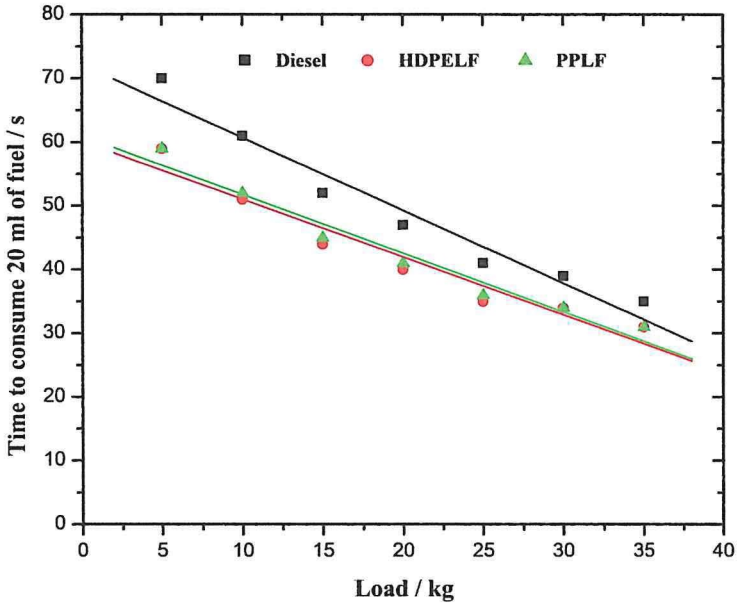

Figure 4.8: Variation of time to consume 20 ml of fuel with engine load

The specific fuel consumption was assessed to determine the length of time that the fuel sample last or can be consumed by the engine. It is observed that the time for the engine to consume 20 ml of fuel sample decreases with an increase in engine load. The engine took a much longer time to consume 20 ml of standard diesel fuel than HDPELF and PPLF at all loads. This is attributed to the greater density of standard diesel compared

to the density of HDPELF and PPLF. Fuels with higher density generally have a higher energy content per unit volume. This means that a smaller volume of high-density fuel can contain the same or more energy compared to a larger volume of low-density fuel. Consequently, if the energy requirements remain constant, using high-density fuel would result in longer consumption times compared to low-density fuel, as it provides more energy per unit volume.

Regression analysis was performed for the time to consume 20 ml of fuel and engine load, the P-values determined at 95 % confidence level were 0.00015, 0.00029, and 0.000096 for standard diesel, HDPELF, and PPLF respectively as shown in APPENDIX E. These values are less than 0.05 implying that there is a significant relationship between the time of consumption of fuel and engine load.

4.4.2 Engine speed

When engine conditions were steady, the engine speed at different engine loads was recorded as shown in Table C.1 (APPENDIX C) from which a graph of engine speed against engine load was obtained as shown in Figure 4.9.

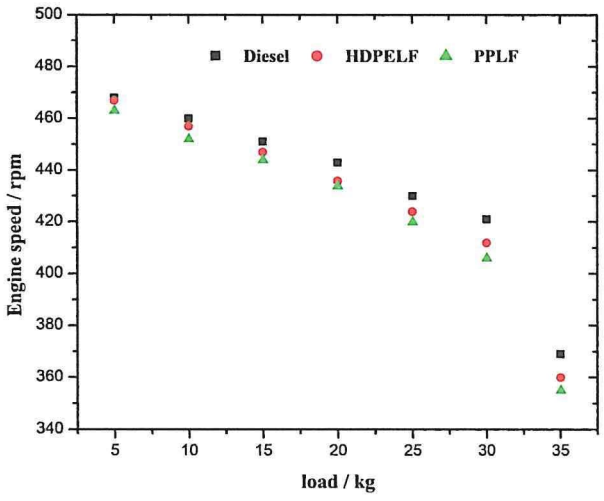

Figure 4.9: Variation of engine speed with load

It is observed that engine speed decreases with an increase in engine load. As the engine load increases, more power is required to overcome resistance or perform work, the

engine speed tends to decrease. This decrease in speed is due to the increase in load, demanding more power from the engine. Therefore, the engine responds by reducing its speed to generate more torque and deliver the necessary power output (Ferrari et al., 2022). The engine speed was correlated with engine load using linear regression analysis. From the regression analysis, the rate at which engine speed decreases with an increase in engine load when using standard diesel, HDPELF, and PPLF is 84.7 %, 87.6 %, and 87.5 % respectively. This reveals that the rate at which engine speed decreases when using standard diesel is lower than when using liquid fuel from plastic waste.

The p – values obtained at 95 % confidence level were 0.0033, 0.0019, and 0.0019 for standard diesel, HDPELF, and PPLF respectively as shown in APPENDIX H. These values are less than 0.05 significance level, indicating that engine speed is statistically significant with engine load.

4.4.3 Mass flow rate of the fuel

The fuel mass flow rate of standard diesel, HDPELF, and PPLF was calculated using equation 3.5 and then recorded as shown in Table C.2 (APPENDIX C) from which a graph of mass flow rate against engine load was obtained as shown in Figure 4.10.

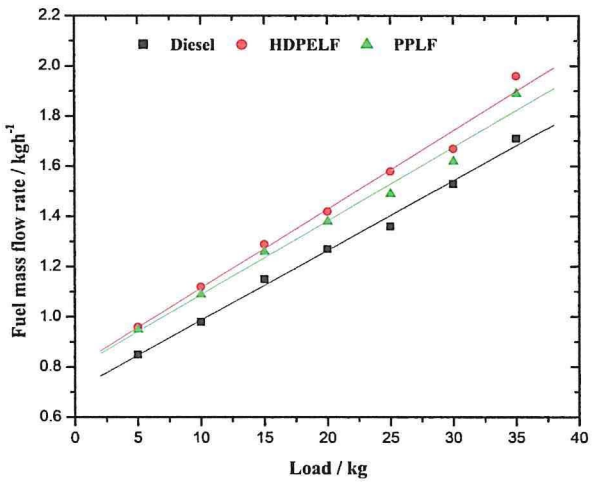

Figure 4.10: Variation fuel mass flow rate with engine load

It has been found that an increase in engine load results in an increase in the fuel mass

flow rate. As the engine load increases, more power output is required, resulting in an increased fuel mass flow rate. Higher engine loads demand more fuel to meet the increased power demands (Heywood, 2018). High-density polyethylene liquid fuel and polypropylene liquid fuel exhibited a higher fuel mass flow rate at all engine loads than standard diesel. This is due to the lower density of HDPELF and PPLF compared to that of standard diesel fuel. The mass flow rate is directly proportional to the fuel density (equation 3.7). The fuel mass flow rate increases if the density of the fuel increases, assuming all other factors remain constant. Similarly, if the density of the fuel decreases, the mass flow rate decreases. The fuel mass flow rate affects the combustion efficiency of the engine. An appropriate fuel-air ratio is necessary for efficient combustion. Insufficient fuel flow can result in a lean mixture, leading to incomplete combustion and reduced efficiency (Stone, 1999). Conversely, excessive fuel flow can lead to a rich mixture, resulting in incomplete combustion, increased fuel consumption, and higher emissions. Fuel mass flow rate also directly affects the power output of an engine. Increasing the fuel mass flow rate allows the engine to burn more fuel and produce more energy, resulting in higher power output.

Using regression analysis, the p – values obtained are 0.0000011, 0.0000072, and 0.000011 respectively. These values are less than 0.05 significance level, implying that there exists a statistical significance between fuel mass flow rate and engine load.

4.4.4 Brake power

The fuel's Brake power was calculated using equation 3.8 and recorded as shown in Table D.1 (APPENDIX D), from which Figure 4.11 was obtained. It is observed from Figure 4.11 that the engine brake power increased with an increase in engine load until a certain point where the brake power was maximum and then started to decrease with an increase in load. At 5 kg engine load, the brake power produced by HDPELF was equal to that produced by standard diesel, and the brake power produced by PPLF was lower than that of standard diesel by about 0.826 %. At 35 kg engine load, the engine brake power produced by HDPELF and PPLF dropped by 2.46 % and 3.84 % respectively compared to that produced by standard diesel.

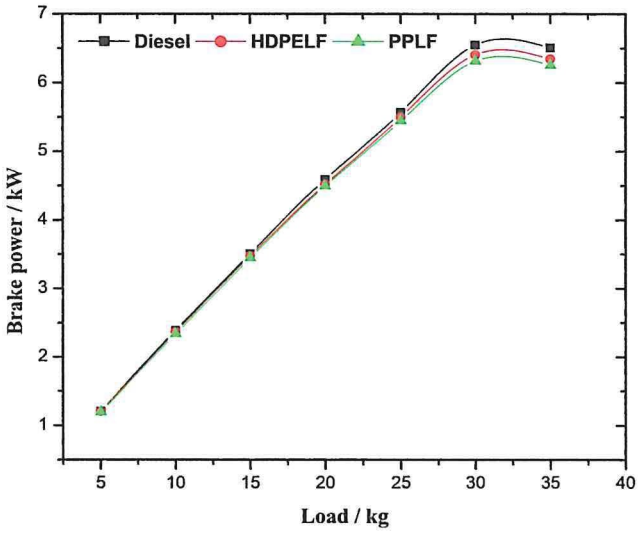

Figure 4.11: Variation of Brake power with engine load

Standard diesel fuel is designed to burn efficiently in diesel engines. This trend of brake power is attributed to diesel engines which are specifically designed to optimize the combustion process with diesel fuel, including factors such as injection timing, air-fuel ratio, and combustion chamber design. This results in a more complete and efficient combustion process, which translates into higher brake power. In contrast, liquid fuel derived from HDPE and PP plastics have different combustion characteristics and may not be as well-matched to the engine design, leading to reduced combustion efficiency and lower brake power. Besides this variation, HDPELF and PPLF can be a better supplement to the existing fossil fuels in terms of brake power.

4.4.5 Brake specific fuel consumption

Brake-specific fuel consumption was calculated from brake power and fuel mass flow rate using equation 3.9 and recorded as shown in Table D.2 (APPENDIX D). A graph of BSFC was obtained as shown in Figure 4.12. It is observed that the brake-specific fuel consumption of all the fuel samples was high at low loads. It decreased with an increase in engine load up to about 30 kg and started to increase. This variation is due to the gradual improvement in the fuel combustion process that increases total energy utilization (Hadi et al., 2020). At higher loads, the cylinder temperature increases resulting in better fuel

combustion and less fuel consumption (Harish and Kempaiah, 2020)

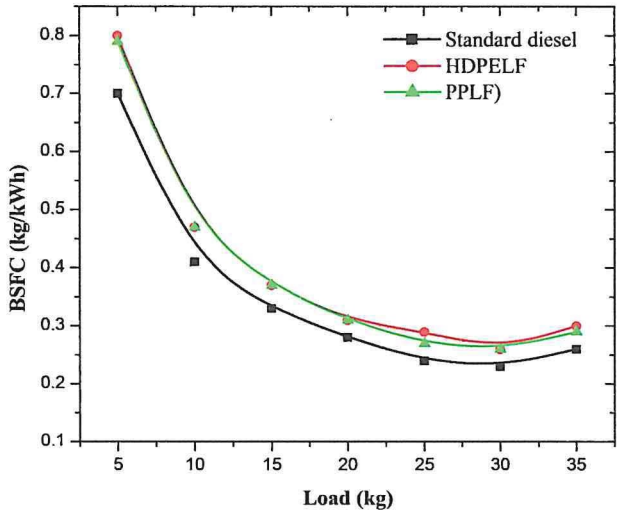

Figure 4.12: Variation of BSFC with engine load

The BSFC data were analyzed using regression with a polynomial fit of degree 5. Using the R squared values, it was observed that the BSFC of standard diesel was decreasing at a rate of 67.4 % with an increase in engine load, while HDPELF and PPLF indicated a lower rate of decrease in BSFC of 64.7 % and 66.6 % respectively with an increase in engine load. The lower BSFC attained for standard diesel fuel at all engine loads compared to HDPELF and PPLF is attributed to its higher density. The average BSFC for HDPELF and PPLF at all engine loads was higher than that of standard diesel by 12.8 % and 10.7 % respectively.

From the regression analysis, BSFC was tested at 95 % confidence level as shown in Table APPENDIX G. The P-values obtained are 0.0236, 0.0288, and 0.0252 for standard diesel, HDPELF, and PPLF respectively. These values are less than 0.05 significance level indicating that there is statistical significance between BSFC and engine load.

4.4.6 Brake Thermal Efficiency

Brake thermal efficiency was calculated using equation 3.9 and recorded as shown in Table D.3 (APPENDIX D) from which a graph of BTE against engine load was obtained as shown in Figure 4.13.

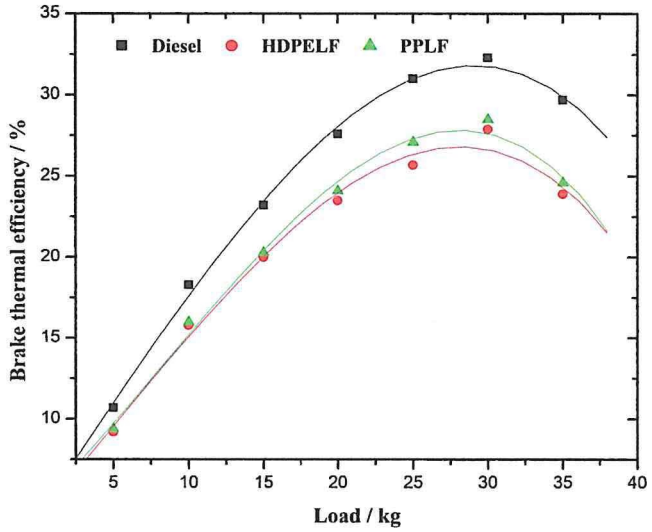

Figure 4.13: Variation of Brake thermal efficiency with load

It is observed that brake thermal efficiency is lower at low engine load. This is attributed to a higher air-fuel ratio leading to incomplete flame propagation which leaves most of the charges unburnt (Kumar et al., 2016). As the engine load increased, the BTE increased because of complete fuel combustion as a result of an increase in the air-fuel ratio. Higher brake thermal efficiency for standard diesel compared to HDPELF and PPLF was observed. The BTE for standard diesel, PPLF, and HDPELF at the 30 kg load are 32.3 %, 28.5 %, and 27.9 % respectively. BTE increases with an increase in engine load.

Using regression analysis and polynomial fit of the third order, the BTE of the engine was analyzed for the three fuel samples with respect to engine load as shown in APPENDIX H. The results revealed that the rate at which BTE increased with an increase in engine load was 91.2 % when using standard diesel compared to 88.2 % when using HDPELF and PPLF fuel samples. The p-values obtained are 0.0042, 0.0086, and 0.0085. These values are less than 0.05 significance level at 95 % confidence level indicating that there is a statistical significance between BTE and engine load.

Chapter 5

Conclusion and Recommendations

5.1 Conclusion

The study focused on evaluating the performance of plastic-derived fuel in a compression ignition engine. The liquid fuel was produced from PP and HDPE plastics through thermal pyrolysis using a fabricated pyrolysis system, in the absence of a catalyst. The liquid fuel obtained was characterized based on its properties and performance in a CI engine.

The fabricated pyrolysis system was used to produce liquid fuel from plastics. After 3 hours of heating PP plastics, 79.8 % liquid fuel, 2.6 % solid residue, and 17.6 % gaseous product were recovered. A maximum of 81.2 % liquid fuel, 5.8 % solid residue, and 13.0 % gaseous product were recovered from HDPE plastic after 3 hours and 20 minutes of heating.

The density of HDPE and PP liquid fuel compared to the required range of 0.817 – 0.867 g cm^{-3} at 15 ^{o}C was 0.790 ± 0.003 and 0.788 ± 0.001 g cm^{-3} using ASTM D1298 test method. The ash content was found to be 0.03 ± 0.01 and 0.02 ± 0.00 % (m/m) using ASTM D482 test method but greater than the allowed maximum value of 0.01 % (m/m) for automotive diesel. The kinematic viscosity was 2.00 ± 0.04 and 2.04 ± 0.02 cSt using ASTM D445, cetane index was found to be 65 and 66 respectively using ASTM D976.The corrosiveness of HDPELF was class 3a while that of PPLF was class 1a based on ASTM D130 test method. The volume of HDPLF and PPLF recovered at 250 ^{o}C and 350 ^{o}C during distillation conform to standard diesel as indicated in ASTM D86 test method. The calorific values were found to be 48.65 and 48.52 MJ/kg for HDPELF and PPLF respec-

tively higher than the 47.59 MJ/kg of standard diesel.

The engine performance tests show that liquid fuel from HDPE and PP plastics has 12.8 % and 10.7 % higher brake-specific fuel consumption than that of standard diesel, while the brake power was lower by 1.3 % and 2.3 % compared to when standard diesel was used.

In conclusion, the liquid fuel obtained from HDPE and PP plastics can be used as an alternative fuel in diesel engines, with a minimum drop in brake power. However, its consumption is higher than that of standard diesel fuel in an engine.

5.2 Recommendations

Based on the findings of this study, further research is recommended to;
Examine the effects of blending plastic-derived fuel with standard diesel and explore the potential of incorporating additives to improve fuel properties and engine performance. Investigate the impact of different fuel blends on combustion characteristics, emissions, and engine efficiency. Optimize blending ratios to maximize performance while meeting regulatory requirements.

Conduct detailed combustion analysis to understand the combustion behavior of plastic-derived fuel in a CI engine. Investigate ignition delay, combustion duration, heat release rate, and flame propagation characteristics. Evaluate the emissions profile of the plastic-derived fuel compared to standard diesel fuel under various engine operating conditions.

Investigate the impact of plastic-derived fuel on engine durability and wear. Analyze engine components for signs of degradation, deposits, and corrosion resulting from prolonged use of plastic-derived fuel. Assess lubricity and the potential for engine damage due to impurities or contaminants in the fuel.

Conduct real-world field testing of vehicles or equipment using plastic-derived fuel to assess performance and emissions under actual operating conditions. Gather data on fuel consumption, engine reliability, and exhaust emissions to validate laboratory findings.

References

Altohami, E. K. and Mustafa, M. A. (2018). Effect of kaolin as a catalyst on the yield of catalytic pyrolysis of waste plastic mixtures. *UofKEJ*, 2:17–24.

ASTM, ASTM, I. (2003). *Annual Book of ASTM Standards*. ASTM International.

Atkins, R. (2009). *An introduction to engine testing and development*. SAE International.

Baines, J. T. (1993). *New Zealand energy information handbook: energy data, conversion factors, definitions*. Taylor Baines and Associates.

Bradfield, F. L. (2014). *Examination of the thermal properties of municipal solid waste and the scalability of its pyrolysis*. PhD thesis, Stellenbosch: Stellenbosch University.

Brebu, M., Bhaskar, T., Murai, K., Muto, A., Sakata, Y., and Uddin, M. A. (2004). The effect of pvc and/or pet on thermal degradation of polymer mixtures containing brominated abs. *Fuel*, 83(14-15):2021–2028.

Bulushev, D. A. and Ross, J. R. (2018). Heterogeneous catalysts for hydrogenation of co2 and bicarbonates to formic acid and formates. *Catalysis Reviews*, 60(4):566–593.

Chomba, E. M. (2018). *Pyrolysis of waste plastics into chemicals as an alternative to landfilling or incineration*. PhD thesis, Stellenbosch: Stellenbosch University.

Coniwanti, P., Sakinah, I. N., Hadiah, F., Putri, F. U. K., Muin, R., et al. (2020). The effect of cracking temperature from a mixture of hdpe and ldpe type plastic waste using zeolite catalyst on the quality of liquid fuel products. In *Journal of Physics: Conference Series*, volume 1500, page 012088. IOP Publishing.

Council, R. D. (2017). Different types of plastic and their classification.

Demirbas, A. (2004). Pyrolysis of municipal plastic wastes for recovery of gasoline-range hydrocarbons. *Journal of Analytical and Applied Pyrolysis*, 72(1):97–102.

Dobó, Z., Jakab, Z., Nagy, G., Koós, T., Szemmelveisz, K., and Muránszky, G. (2019). Transportation fuel from plastic wastes: production, purification and si engine tests. *Energy*, 189:116353.

Ferrari, G., Onorati, A., and D'Errico, G. (2022). *Internal combustion engines*. Società Editrice Esculapio.

George, E., Rajesh, S., and David, F. (2003). Fuels and lubricants handbook: technology, properties, performance, and testing. *Astm International, USA*, page 224.

Hadi, A. S., Ahmed, O. K., and Ali, O. M. (2020). Enhancement of gasoline fuel quality with commercial additives to improve engine performance. In *IOP Conference Series: Materials Science and Engineering*, volume 745, page 012065. IOP Publishing.

Harish, H. and Kempaiah, U. (2020). Experimental investigation on performance and emission of ci engine using b20 waste cooking oil with and without exhaust gas recirculation. In *AIP Conference Proceedings*, volume 2247, page 030002. AIP Publishing LLC.

Heywood, J. B. (2018). *Internal combustion engine fundamentals*. McGraw-Hill Education.

Jain, P., Patidar, B., and Bhawsar, J. (2020). Potential of nanoparticles as a corrosion inhibitor: a review. *Journal of Bio-and Tribo-Corrosion*, 6:1–12.

Khan, M., Sultana, M., Al-Mamun, M., and Hasan, M. (2016). Pyrolytic waste plastic oil and its diesel blend: fuel characterization. *Journal of environmental and public health*, 2016.

Kumar, A., Shukla, S., and Tirkey, J. (2016). Performance and emission characteristics of coconut biodiesel and diesel blends on vcr engine. *Int J Inno Res EngMana (IJIREM)*, 3:381–390.

Kyaw, K. T. and Hmwe, C. S. S. (2015). Effect of various catalysts on fuel oil pyrolysis process of mixed plastic wastes. *International Journal of Advances in Engineering & Technology*, 8(5):794.

Macharia, E. M. (2018). *A study of waste plastic oil as an alternative fuel to diesel in compression ignition engines*. PhD thesis, University of Nairobi.

Malinović, B., Borković, A., and uričić, T. (2022). Copper strip corrosion testing in hydrocracked base oil in the presence of different inhibitors. *HEMIJSKA INDUSTRIJA (Chemical Industry)*, 76(3):159–166.

Mangesh, V., Padmanabhan, S., Ganesan, S., PrabhudevRahul, D., and Reddy, T. D. K. (2017). Prospects of pyrolysis oil from plastic waste as fuel for diesel engines: A review. In *IOP Conference Series: Materials Science and Engineering*, volume 197, page 012027. IOP Publishing.

Marcilla, A., del Remedio Hernández, M., and García, Á. N. (2007). Study of the polymer–catalyst contact effectivity and the heating rate influence on the hdpe pyrolysis. *Journal of analytical and applied pyrolysis*, 79(1-2):424–432.

Miskolczi, N., Bartha, L., and Angyal, A. (2009). Pyrolysis of polyvinyl chloride (pvc)-containing mixed plastic wastes for recovery of hydrocarbons. *Energy & Fuels*, 23(5):2743–2749.

Miskolczi, N., Bartha, L., Deák, G., Jóver, B., and Kallo, D. (2004). Thermal and thermocatalytic degradation of high-density polyethylene waste. *Journal of Analytical and Applied Pyrolysis*, 72(2):235–242.

Moses, K. (2014). *Production and Characterization of Liquid Fuel from Mixed Plastic Wastes Using Catalytic Pyrolysis*. PhD thesis, Makerere University Kampala, Uganda.

Nadkarni, R. and Nadkarni, R. (2007). *Guide to ASTM test methods for the analysis of petroleum products and lubricants*, volume 44. ASTM International West Conshohocken.

Olufemi, A. and Olagboye, S. (2017). Thermal conversion of waste plastics into fuel oil. *Int J Petrochem Sci Eng*, 2(8):252–257.

Owusu, P. A., Banadda, N., Zziwa, A., Seay, J., and Kiggundu, N. (2018). Reverse engineering of plastic waste into useful fuel products. *Journal of Analytical and Applied Pyrolysis*, 130:285–293.

Padsalgikar, A. (2017). *Plastics in medical devices for cardiovascular applications*. William Andrew.

Quesada, L., Calero, M., Martín-Lara, M., Pérez, A., and Blázquez, G. (2019). Characterization of fuel produced by pyrolysis of plastic film obtained of municipal solid waste. *Energy*, 186:115874.

Sabarinath, S., Rajendrakumar, P., and Prabhakaran Nair, K. (2019). Evaluation of tribological properties of sesame oil as biolubricant with sio2 nanoparticles and imidazolium-based ionic liquid as hybrid additives. *Proceedings of the Institution of Mechanical Engineers, Part J: Journal of Engineering Tribology*, 233(9):1306–1317.

Sakata, Y., Uddin, M. A., Koizumi, K., and Murata, K. (1996). Thermal degradation of polyethylene mixed with poly (vinyl chloride) and poly (ethyleneterephthalate). *Polymer Degradation and Stability*, 53(1):111–117.

Sayyed, S., Das, R. K., and Kulkarni, K. (2021). Performance assessment of multiple biodiesel blended diesel engine and nox modeling using ann. *Case Studies in Thermal Engineering*, 28:101509.

Singhabhandhu, A. and Tezuka, T. (2010). The waste-to-energy framework for integrated multi-waste utilization: Waste cooking oil, waste lubricating oil, and waste plastics. *Energy*, 35(6):2544–2551.

Stone, R. (1999). *Introduction to internal combustion engines*, volume 3. Springer.

Suresh, M., Jawahar, C., and Richard, A. (2018). A review on biodiesel production, combustion, performance, and emission characteristics of non-edible oils in variable compression ratio diesel engine using biodiesel and its blends. *Renewable and Sustainable Energy Reviews*, 92:38–49.

Thahir, R., Altway, A., Juliastuti, S. R., et al. (2019). Production of liquid fuel from plastic waste using integrated pyrolysis method with refinery distillation bubble cap plate column. *Energy reports*, 5:70–77.

Tiseo, I. (2021). Annual production of plastics worldwide from 1950 to 2020 (in million metric tons). *statista-The statistical portal. Retrieved on September*, 10:2021.

Tsakona, M. and Rucevska, I. (2020). Baseline report on plastic waste. *UNEP https://gridarendalwebsite-live. s3. amazonaws. com/production/documents/: s_document/554/original/UNEPCHW-PWPWG.*

Tulashie, S. K., Boadu, E. K., and Dapaah, S. (2019). Plastic waste to fuel via pyrolysis: A key way to solving the severe plastic waste problem in ghana. *Thermal Science and Engineering Progress*, 11:417–424.

UNBS (2019). Draft east africa standard for automotive gas oil (automotive diesel) — specification.

Van Gerpen, J., Shanks, B., Pruszko, R., Clements, D., and Knothe, G. (2004). Biodiesel analytical methods: August 2002–january 2004. Technical report, National Renewable Energy Lab., Golden, CO (US).

Wright, E. C. and Purday, H. F. P. (1950). *Diesel Engine Fuels and Lubricants*. Constable.

Appendix A

Residence time and pyrolysis temperature

Table A.1: Residence time and Pyrolysis temperature for PP plastics

t/min	T/°C	t/min	T/°C	t/min	T/°C	t/min	T/°C	t/min	T/°C	t/min	T/°C
0	34	31	309.4	62	358.7	93	313.9	124	344.3	155	375.3
1	40	32	307.4	63	336.3	94	319.3	125	340.3	156	388.3
2	49.7	33	306.9	64	333.3	95	325.4	126	336.8	157	396.6
3	65.9	34	306.9	65	334.2	96	330.0	127	335.3	158	406.3
4	80.1	35	304.1	66	334.2	97	334.5	128	334.0	159	411.3
5	98.6	36	304.3	67	334.2	98	335.3	129	332.9	160	409.4
6	116.5	37	304.8	68	332.4	99	334.1	130	336.3	161	408.7
7	133.2	38	304.8	69	332.8	100	329.8	131	337.0	162	402.6
8	148.6	39	304.7	70	332.4	101	325.6	132	338.2	163	398.8
9	162.5	40	305.9	71	330.9	102	320.9	133	334.0	164	403.0
10	174.4	41	306.4	72	330.8	103	317.2	134	336.0	165	401.3
11	188.2	42	310.7	73	331.3	104	312.6	135	337.9	166	403.7
12	201.9	43	313.6	74	325.2	105	309.1	136	343.6	167	402.3
13	213.4	44	315.6	75	321.4	106	321.5	137	348.0	168	401.2
14	222.3	45	315.1	76	319.5	107	330.9	138	349.0	169	402.9
15	235.1	46	317.8	77	315.8	108	333.1	139	352.0	170	405.9
16	239.4	47	325.1	78	315.1	109	338.8	140	349.7	171	410.6
17	247.9	48	327.4	79	312.9	110	339.8	141	346.2	172	410.4
18	254.1	49	327.4	80	310.1	111	339.0	142	342.9	173	410.8
19	260.4	50	326.6	81	310.1	112	334.9	143	337.6	174	410.8
20	264.0	51	327.0	82	309.3	113	329.7	144	333.3	175	410.8
21	268.1	52	327.5	83	316.8	114	322.4	145	320.9	176	410.8
22	275.2	53	326.1	84	322.3	115	317.9	146	316.6	177	410.8
23	281.4	54	324.3	85	321.5	116	312.2	147	303.8	178	410.8
24	285.3	55	325.1	86	321.4	117	315.9	148	302.6	179	410.8
25	292.3	56	329.3	87	317.3	118	317.3	149	295.3	180	410.8
26	298.5	57	332.1	88	318.0	119	318.4	150	290.4		
27	306.3	58	330.5	89	318.3	120	326.8	151	296.4		
28	309.0	59	324.9	90	317.3	121	336.3	152	307.5		
29	311.2	60	323.4	91	317.5	122	342.9	153	330.8		
30	310.6	61	340.4	92	315.2	123	344.1	154	349.6		

Table A.2: Residence Time and Pyrolysis Temperature for HDPE plastics

t/min	T/°C	t/min	T/°C	t/min	T/°C	t/min	T/°C	t/min	T/°C	t/min	T/°C	t/min	T/°C
0	27	31	319.4	62	330.4	93	327.3	124	337.2	155	356.8	186	417.8
1	34	32	318.9	63	333.2	94	327.7	125	341.2	156	357.9	187	418.3
2	40.9	33	318.2	64	334.6	95	328.1	126	340.3	157	359.9	188	418.2
3	55.8	34	316.8	65	334.9	96	330.8	127	339.7	158	366.8	189	418.9
4	68.9	35	316.7	66	334.8	97	334.3	128	337.8	159	369.5	190	418.8
5	79.9	36	317.1	67	334.7	98	335.3	129	335.2	160	371.3	191	418.9
6	96.4	37	316.0	68	335.1	99	334.1	130	336.2	161	377.8	192	418.0
7	112.8	38	318.6	69	334.6	100	332.9	131	338.0	162	380.2	193	418.0
8	139.7	39	318.9	70	334.8	101	331.8	132	338.4	163	389.7	194	418.0
9	152.0	40	319.8	71	335.8	102	330.3	133	336.4	164	393.8		
10	169.1	41	320.3	72	335.4	103	329.3	134	336.0	165	397.6		
11	178.6	42	322.4	73	335.9	104	326.6	135	337.7	166	400.3		
12	193.7	43	324.6	74	335.1	105	325.4	136	343.6	167	403.0		
13	213.0	44	324.8	75	335.7	106	326.9	137	346.2	168	403.9		
14	224.3	45	324.9	76	335.8	107	328.9	138	348.6	169	403.7		
15	234.9	46	325.3	77	336.2	108	332.8	139	354.3	170	403.6		
16	240.3	47	325.1	78	335.8	109	338.8	140	355.0	171	402.8		
17	250.4	48	327.7	79	336.3	110	337.9	141	356.8	172	404.6		
18	254.1	49	327.1	80	336.9	111	339.7	142	357.3	173	406.2		
19	257.9	50	326.6	81	336.4	112	338.2	143	354.3	174	405.9		
20	259.8	51	327.0	82	335.9	113	338.1	144	352.1	175	407.1		
21	260.7	52	327.3	83	335.3	114	337.1	145	348.8	176	408.3		
22	264.7	53	326.1	84	335.8	115	330.8	146	347.9	177	409.1		
23	268.9	54	324.3	85	334.9	116	327.7	147	348.5	178	410.5		
24	273.4	55	325.1	86	334.7	117	326.4	148	348.9	179	411.0		
25	277.7	56	329.3	87	334.2	118	326.7	149	347.3	180	411.9		
26	284.3	57	332.1	88	333.9	119	325.9	150	348.9	181	412.2		
27	292.0	58	330.5	89	332.4	120	326.7	151	349.8	182	412.9		
28	306.3	59	324.9	90	332.9	121	329.7	152	350.0	183	413.7		
29	312.1	60	323.4	91	329.8	122	334.6	153	352.6	184	413.9		
30	313.5	61	328.2	92	327.9	123	336.8	154	353.5	185	414.9		

Appendix B

Fuel properties

Table B.1: Distillation characteristics of diesel and liquid fuel from plastics

Percent Recovered %(V/V)	Observed Temperature /°C		
	Diesel	HDPELF	PPLF
0	175.2	134.7	110.1
5	200.5	158.4	132.0
10	209.1	171.6	140.1
15	220.2	184.7	149.9
20	228.8	196.9	160.3
25	235.9	208.0	170.5
30	241.9	217.1	183.6
35	249.5	230.3	202.8
40	256.6	238.3	222.7
45	263.2	247.5	239.3
50	269.2	255.5	253.1
55	276.3	264.6	266.2
60	283.9	273.2	280.7
65	291.0	280.8	295.9
70	299.1	288.9	312.8
75	307.2	297.5	326.9
80	316.3	309.7	340.8
85	326.9	319.8	354.6
90	338.0	335.0	362.3
95	354.2	352.7	365.4
100	359.3	365.3	366.7

Table B.2: Analysed fuel properties and their acceptable range

Property	Diesel	HDPELF	PPLF	Accepted	Method
Density at 15°C / gcm^{-3}	0.830	0.790	0.788	0.820-0.870	ASTM D1298
Kinematic viscosity at 40°C/cSt	2.7	2.0	2.0	2.0-5.3	ASTM D445
Calorific value/ $MJkg^{-1}$	47.59	48.65	48.52	-	IKA C2000
Ash content %(m/m)	0.02	0.03	0.02	≤ 0.01	ASTM D482
Cetane index	53	65	66	≥ 48	ASTM D976
Copper strip corrosion/Rating	1a	3a	1a	class 1	ASTM D130
Distillation					ASTM D86
(a) IBP/°C	175	135	110	-	
(b) % recovered at 250°C	41.0	51.0	52.0	≤ 65	
(c) % recovered at 350°C	96.0	95.0	87.0	≥ 85	
(d) 95% recovery/°C	354	352	365	≤ 360	
(e) FBP/°C	359	365	366	≤ 400	

Appendix C

Engine performance tests

Table C.1: Engine speed and consumption time at different load.

Load/kg	Speed, N/rpm			Time, *t*/s		
	Diesel	**HDPELF**	**PPLF**	**Diesel**	**HDPELF**	**PPLF**
5	468	467	463	70	59	59
10	460	457	452	61	51	52
15	451	447	444	52	44	45
20	443	436	434	47	40	41
25	430	424	420	41	35	36
30	421	412	406	39	34	34
35	369	360	355	35	31	31

Table C.2: Fuel mass flow rate.

Load/kg	Mass flow rate/ kgh^{-1}		
	Diesel	**HDPELF**	**PPLF**
5	0.85	0.96	0.95
10	0.98	1.12	1.09
15	1.15	1.29	1.26
20	1.27	1.42	1.38
25	1.36	1.58	1.49
30	1.53	1.67	1.62
35	1.71	1.96	1.89

Appendix D

Engine performance parameters

Table D.1: Brake power produced by the engine at different loads

Load/kg	Brake power/kW		
	Diesel	HDPELF	PPLF
5	1.21	1.21	1.20
10	2.39	2.37	2.34
15	3.51	3.48	3.45
20	4.39	4.52	4.50
25	5.57	5.50	5.45
30	6.55	6.41	6.32
35	6.51	6.35	6.26

Table D.2: Brake Specific Fuel Consumption at different loads

Load/kg	BSFC/kg$(kWh)^{-1}$		
	Diesel	HDPELF	PPLF
5	0.70	0.80	0.79
10	0.41	0.47	0.47
15	0.33	0.37	0.37
20	0.28	0.31	0.31
25	0.24	0.29	0.27
30	0.23	0.26	0.26
35	0.26	0.31	0.30

Table D.3: Brake thermal efficiency at different engine load

Load/kg	BTE/%		
	Diesel	HDPELF	PPLF
5	10.7	9.2	9.4
10	18.3	15.8	16.0
15	23.2	20.0	20.3
20	27.6	23.5	24.1
25	31.0	25.7	27.1
30	32.3	27.9	28.5
35	29.7	23.9	24.6

Appendix E

Regression analysis for time to consume 20 ml with engine load

Table E.1: Regression analysis for time to consume 20 ml of standard diesel

	Coefficients	Standard error	t Stat	P-value	R squared
intercept	72.1428571	2.482592457	29.0594846	9E-07	0.9549
Standard diesel	-1.1428571	0.11102491	-10.2937	0.00015	

Table E.2: Regression analysis for for time to consume 20 ml of HDPELF

	Coefficients	Standard error	t Stat	P-value	R squared
intercept	60.14285714	2.266661665	26.533672	1.42145E-06	0.9412
HDPELF	-0.907142857	0.101368191	-8.94898928	0.000290414	

Table E.3: Regression analysis for for time to consume 20 ml of PPLF

	Coefficients	Standard error	t Stat	P-value	R squared
intercept	61	1.828069127	33.3685412	4.5441E-07	0.9621
PPLF	-0.92142857	0.081753737	-11.2707823	9.6069E-05	

Appendix F

Regression analysis for fuel mass flow rate with engine load

Table F.1: Regression analysis for mass flow rate of standard diesel

	Coefficients	Standard error	t Stat	P-value	R squared
intercept	0.70857143	0.022485823	31.5119	6.04303E-07	0.9935
Standard diesel	0.02778571	0.001005597	27.6311	1.16209E-06	

Table F.2: Regression analysis for mass flow rate of HDPELF

	Coefficients	Standard error	t Stat	P-value	R squared
intercept	0.80142857	0.036638053	21.8742128	3.70651E-06	0.9865
HDPELF	0.031335714	0.001638504	19.1376716	7.18186E-06	

Table F.3: Regression analysis for mass flow rate of PPLF

	Coefficients	Standard error	t Stat	P-value	R squared
intercept	0.79571429	0.037518703	21.2084701	4.31984E-06	0.9839
PPLF	0.02935714	0.001677887	17.4964916	1.11807E-05	

Appendix G

Regression analysis for BSFC with engine load

Table G.1: Regression analysis for BSFC using standard diesel

	Coefficients	Standard error	t Stat	P-value	R squared
intercept	0.60285714	0.087920999	6.85680498	0.0010081	0.6740
Standard diesel	-0.0126429	0.003931847	-3.2154193	0.0235858	

Table G.2: Regression analysis for BSFC using HDPELF

	Coefficients	Standard error	t Stat	P-value	R squared
intercept	0.68285714	0.103566502	6.59341705	0.0012058	0.6486
HDPELF	-0.0140714	0.004631635	-3.0381127	0.0288129	

Table G.3: Regression analysis for BSFC using PPLF

	Coefficients	Standard error	t Stat	P-value	R squared
intercept	0.68	0.100668683	6.75483161	0.00108	0.6660
PPLF	-0.0142143	0.00450204	-3.1572986	0.02517	

Appendix H

Regression analysis for BTE with engine load

Table H.1: Regression analysis for BTE using standard diesel

	Coefficients	Standard error	t Stat	P-value	R squared
intercept	11.4286	2.9881	3.8246	0.0123	0.9116
Standard diesel	0.6629	0.1336	4.9603	0.0042	

Table H.2: Regression analysis for BTE using HDPELF

	Coefficients	Standard error	t Stat	P-value	R squared
intercept	10.2857	2.8266	3.6390	0.0149	0.8818
HDPELF	0.5286	0.1264	4.1815	0.0086	

Table H.3: Regression analysis for BTE using PPLF

	Coefficients	Standard error	t Stat	P-value	R squared
intercept	10.3714	2.9481	3.5180	0.0170	0.8824
PPLF	0.5529	0.1318	4.1933	0.0085	